agronomy

MDPI

Article

Limits of Conventional Management for Carbon Sequestration Across a Semi-Arid Mediterranean Agricultural Region: The Valencian Community

José Miguel de Paz [1], Domingo José Iglesias [2], Sara Miguel [1,3], Enrique Peiró [1] and Fernando Visconti [1,*]

[1] Centro de Agrotecnologías Avanzadas-Unidad de Agricultura Sostenible-CATA-UAS, Instituto Valenciano de Investigaciones Agrarias-IVIA (GVA), Carretera CV-315, km 10.7, 46113 Moncada, València, Spain; depaz_jos@gva.es (J.M.d.P.); miguel_sar@gva.es (S.M.); peiro_enr@gva.es (E.P.)
[2] Centro de Genómica, Instituto Valenciano de Investigaciones Agrarias-IVIA (GVA), Crta. CV-315, km 10.7, 46113 Moncada, València, Spain; iglesias_dom@gva.es
[3] Programa de Doctorado en Recursos y Tecnologías Agrícolas, Universitat Politècnica de València, Camí de Vera s/n, 46022 València, Spain
* Correspondence: visconti_fer@gva.es; Tel.: +34-963424095

Abstract

To develop carbon farming practices, decision-makers need detailed spatial data on the soil carbon sequestration (SCS) opportunities that conventional crop and soil management creates. This study exploratorily assessed SCS capacity across agricultural land in the Valencian Community using a simple carbon balance model within a GIS framework. Within this modelling approach, maps of net primary production (NPP), land-use-derived crop harvest indices, current soil organic carbon (SOC) stocks, and NPP and SOC mineralization coefficients were combined. Results show that while NPP across Valencian croplands and grasslands ranges from 0.64 to 6.43 Mg C ha^{-1} yr^{-1} (mean 2.42 Mg C ha^{-1} yr^{-1}), the actual SCS capacity is much lower, ranging from −0.04 to 1.31 Mg C ha^{-1} yr^{-1} (mean 0.25 Mg C ha^{-1} yr^{-1}). Significant variation exists among land uses: rice paddies exhibit the highest SCS capacity, while olive groves present the lowest. Between 2017 and 2021, SCS in Valencian agroecosystems may have offset the sector's greenhouse gas (GHG) emissions, primarily driven by pasture and citrus because of their large extent and moderate SCS capacity, making agriculture a net-zero emitter. However, helping achieve cross-sectoral mitigation targets will depend in part on the widespread deployment of regenerative soil management (RSM) practices. While this study identifies priority areas for RSM implementation, further research is needed to determine which specific practices are most suitable for each location to maximize SCS.

Keywords: carbon footprint; carbon neutrality; climate change; horticulture; irrigation; LUCAS; MODIS; soil health; viticulture; winegrowing

Academic Editors: Kun Cheng and Qian Yue

Received: 4 March 2026
Revised: 25 March 2026
Accepted: 27 March 2026
Published: 31 March 2026

1. Introduction

Almost 25% of global land is subjected to degradation, resulting in a severe loss of net primary production (NPP) [1], which impairs key soil ecosystem functions such as water cycle regulation, biodiversity reservoir and weather and climate regulation [2]. Erosion by water, compaction, sealing, salinization and the loss of organic carbon constitute the leading soil processes that degrade lands throughout the world [3,4]. These processes increase the desertification risk where, additionally, the conditions of water scarcity are met, since soil water and thermal regimes are the main constraints to land productivity [5].

With nearly 70% of soils classified as unhealthy, Europe is significantly affected by land degradation [6]. In particular, the Mediterranean area, with sloping terrain, arid-to-dry sub-humid climates, high water scarcity in summer and intense seasonal rainfall events, meets the conditions for the most degradative processes to develop, such as water erosion, salinization and, more specifically, the loss of organic carbon, thereby exacerbating soil health decline [7].

In Europe policies are being developed to assess the extent, causes and intensity of land degradation, and to lead actions aimed at improving soil health. With this objective, the European Green Deal with the strategy "from farm to fork" is aimed at reaching climate neutrality in the European Union by 2050 [8]. Within this strategy, agriculture is key for increasing carbon assimilation in plants and, ultimately, carbon sequestration in soils, thereby contributing to the restoration of soil health. Therefore, the proposal for a European Directive on soil monitoring and resilience [9] puts forward the ambitious aim of recovering soil health across Europe by 2050.

The soil organic carbon (SOC) mass fraction (w_{SOC}) and, specifically, the ratio of w_{SOC} to its potential value, is one of the most important indicators of soil health [10]. Moreover, SOC is, apart from the carbonate rocks of the lithosphere, the greatest reservoir of carbon on the Earth's surface [11,12]. At European scale, several soil studies show very low w_{SOC} because of a constant decline in soil organic matter (SOM), particularly in agricultural lands [13–16], thus leading to very low fertility and health status of cropped soils. Specifically, in the Valencian Community (eastern Spain), 64% of agricultural soils present an average topsoil (0–30 cm) SOM mass fraction (w_{SOM}) under a reasonable average 3% potential.

Soils can recover a substantial proportion of their original SOC, thereby improving soil health for enhancing crop yields, while simultaneously reversing carbon losses to the atmosphere with climate change mitigation effects [17]. In this regard, only part of the carbon that plants assimilate is transferred to soil where, depending on management, again, only part is stabilized [18]. This process leads to SOC storage and, more importantly, to soil carbon sequestration (SCS) if SOC is retained over the long-term, specifically at least 100 years [19,20].

Because agriculture can assimilate and potentially sequester substantial amounts of carbon from atmospheric CO_2, it may become a key activity for climate change mitigation. In the context of the current climate crisis, agricultural activity is thus evolving beyond food production to include the development of "carbon farming" practices aimed at offsetting at least part of the anthropogenic CO_2 emissions [21]. Carbon farming may also create new revenue streams for farmers through carbon credit markets, provided that climate integrity requirements are met [22]. In this way, agriculture can assume a dual function, combining productive and environmental roles. Achieving this transition requires replacement of conventional soil management by regenerative practices that enhance soil carbon sequestration while maintaining or even increasing crop yields, thereby fostering a virtuous cycle of mutually reinforcing benefits [17].

The prioritization of agricultural areas for SCS depends on both NPP and on the soil's capacity to stabilize SOC. These factors are, in turn, governed by soil characteristics, climate conditions, land use and crop management, all of which continuously vary across landscapes, therefore making it challenging to accurately assess the SCS capacity of agricultural lands. This complexity is reflected in the wide variability of SCS capacity observed across agricultural landscapes, which range from 0.1 to over 1.0 Mg C ha^{-1} yr^{-1} [23–28]. Consequently, evaluating the SCS capacity across different combinations of soil, climate, land use and crop factors is essential to support decision-makers and land practitioners in the design and implementation of effective policies, strategies and regenerative soil

management (RSM) practices [28]. Moreover, mitigating climate change impacts requires providing decision makers with accurate spatially explicit information on the current state, dynamics, and distribution of carbon sources and sinks within managed territories [29].

At the regional scale, the SCS capacity can be effectively assessed using mapping techniques [30,31], particularly through the coupling or integration of simulation models with Geographical Information Systems (GIS) [32]. Available models range from relatively simple carbon budget approaches [18,24,33–36], typically used for large-scale estimations, to more complex process-based models, such as RothC [37], Century [38], Daycent [39], DNDC [40], etc., which are better suited for detailed, site-specific analyses.

Janzen et al. [18] proposed a simple model for estimating the SCS capacity based on a linear algebraic equation, in which NPP and current SOC stock are the variables, and organic matter translocation and mineralization coefficients are the parameters. Although originally developed to estimate the SCS capacity at global scale, this model can be readily adapted to regional application by means of GIS because of its simplicity and adequate previous performance [18], enabling the exploration of the spatial distribution of the SCS capacity across agricultural regions.

To our knowledge, such an application of Janzen's model has not been undertaken. However, it has the potential to generate valuable insights for tailoring SCS strategies to specific conditions of soil, climate, land use and crop management. This approach is particularly relevant for Mediterranean semi-arid regions, where high spatial variability in SCS capacity has been reported, albeit in still scarce studies [41,42]. Accordingly, the objectives of this research were the following: (i) to conduct an exploratory assessment of the spatial distribution of the SCS capacity across the agricultural land of the Valencian Community (eastern Spain), as a representative semi-arid Mediterranean region, by applying Janzen's model in combination with GIS; and (ii) to examine how the SCS key controlling factors determine its magnitude, thereby providing practical guidance for decision-makers and practitioners engaged in SCS-related efforts.

2. The Model by Janzen et al.

2.1. Model Description

The model by Janzen et al. [18] assesses the SCS in kg C ha^{-1} yr^{-1} as the difference between the *SOC input* minus the *SOC output* (Figure 1):

$$SCS = SOC\ input - SOC\ output = NPP\ (1 - k_1)\ k_2 - SOC\ k_3 \quad (1)$$

The *SOC input* is the fraction of the *NPP* that enters the soil and remains there for at least 5 years. Therefore, the k_1 coefficient stands for the fraction of the *NPP* that is exported out of the agroecosystems in the form of harvest and crop residues and that does not return in the form of recycled plant materials such as manures, sewage sludges, composts, etc., as represented by Equation (2):

$$k_1 = \Sigma_i HI_i + \Sigma_i ERI_i - IOMI \quad (2)$$

In Equation (2), HI_i is the harvest index of the *i*th plant species in the plot, defined as the harvestable biomass of the *i*th plant species divided by its total biomass. *ERIi* is the exported residues index of the *i*th plant species, expressed as the exported residues biomass of the *i*th plant species divided by its total biomass. Finally, *IOMI* is the imported organic matter index, which is expressed as the organic matter that is imported divided by the addition of the biomass of all plants in the plot.

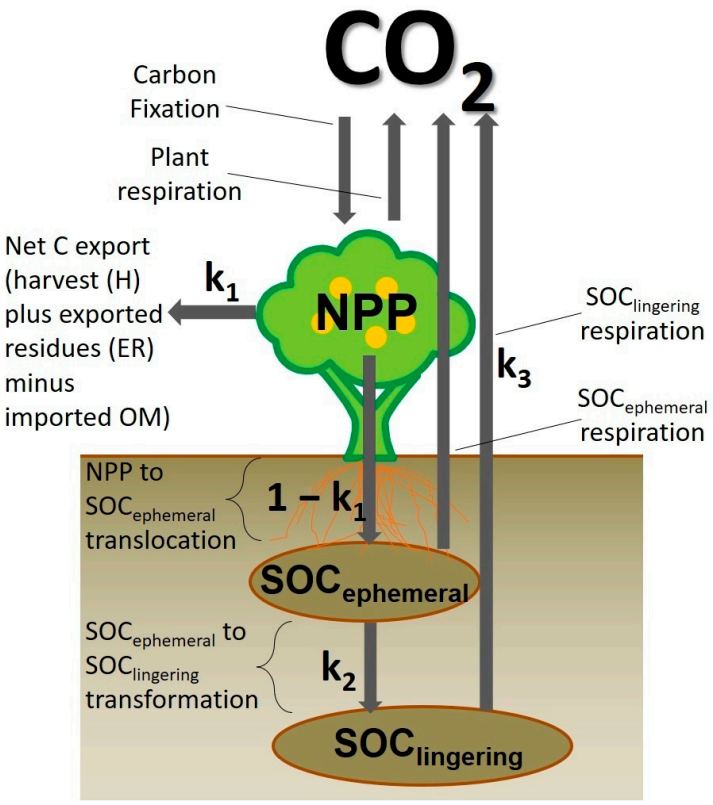

Figure 1. Carbon reservoirs and flows that the model by Janzen et al. [18] uses to estimate the soil carbon sequestration (*SCS*) capacity, in which CO_2 is the atmospheric carbon dioxide reservoir, $SOC_{ephemeral}$ and $SOC_{lingering}$ are, respectively, the short-lived and long-lived, soil organic carbon (SOC) stocks, and k_1, k_2 and k_3 are the coefficients of the model. These represent, respectively, the net ratio of the net primary production (*NPP*) that is drawn from the agroecosystem (k_1), the ratio of the *NPP* that is not drawn and remains in the soil 5 years later (k_2), and the ratio of the SOC stock that is mineralized each year (k_3).

The addition of $\Sigma iHIi$ and $\Sigma_i ERI_i$ is bounded above by 1, i.e., $\Sigma_i HI_i + \Sigma_i ERI_i \in [0, 1]$. For a wide enough land expanse, the average *IOMI* can be regarded as well below the addition of $\Sigma_i HI_i$ and $\Sigma_i ERI_i$, i.e., $IOMI << \Sigma_i HI_i + \Sigma_i ERI_i$, and then $IOMI << 1$. This occurs because the biomass that is exported from crop fields is respired by consumers and decomposers and the remainder is converted to excreta and microbial biomass that takes the form of manures, sewage sludges, composts, etc. These organic materials, upon recirculation to agricultural fields, necessarily make, on average for a large expanse, a comparatively little fraction of the original weight of harvest and crop residues. Therefore, in a plot under agricultural exploitation, the k_1 coefficient may be regarded as bounded between $\Sigma_i HI_i$ and one. Accordingly, $1 - k_1$ represents the fraction of plant biomass that is not removed from the agroecosystem. This fraction may enter the soil as plant residues and rhizodepositions, or, if removed, may be partially returned in the form of manures, sewage sludges, composts, etc.

In this analysis, the concept of plant has been used instead of crop because, for the sake of comprehensiveness, the summations in Equation (2) are extended to all plant species in the plot, including the main crop, as well as cover crops and spontaneous plants. However, under conventional monocropping systems characterized by bare soil between plants and rows, as well as the absence of organic matter recirculation, the biomass source is overwhelmingly the monocrop, such that $\Sigma_i ERI_i \approx 0$ and $IOMI \approx 0$, allowing the analysis to be simplified to

$$k_1 = HI \quad (3)$$

where, additionally, it is considered that no crop residues are withdrawn from the plot, i.e., $ERI \approx 0$:

Following k_1, the k_2 coefficient represents the ratio of the *NPP* entering the soil that remains five years later, which is the timeline that may appropriately serve to separate fast- and slow-decaying SOC, as discussed by Janzen et al. [18]. At the global level, this lingering SOC has been estimated to account for 15% of the *NPP* entering agricultural soils, i.e., $k_2 = 0.15$.

Following the *SOC input*, the *SOC output* (Equation (1)) is the fraction of the SOC that mineralizes over 1 year. Therefore, the k_3 coefficient represents this fraction. It has been estimated that, yearly, 0.2% of the SOC undergoes mineralization in agricultural soils globally, i.e., $k_3 = 0.002$ [43].

2.2. Model Adaptation

The Janzen model was originally developed to obtain a crude estimate of the *SCS* capacity of agriculture at global scale. Therefore, it was not intended to consider the spatial variability of the input data, i.e., both variables (*NPP* and *SOC*) and parameters (k_1, k_2 and k_3). However, in this work, the Janzen model has been adapted to ascertain how the *SCS* capacity spatially varies across a large agricultural area, assuming conventional crop and soil management, and explicitly accounting for the geographical distribution of the Janzen model's variables and parameters. Therefore, this work expands on the original aim of Janzen's model by exploring its capacity for mapping the *SCS* capacity of agricultural lands at regional scale when used within a GIS framework.

3. Material and Methods

3.1. Data Acquisition

The agricultural area of the Valencian Community, comprising both croplands and grasslands, covers 11,135 km^2 [44]. To adapt the model proposed by Janzen et al. [22] to this region, five primary geographic information layers were acquired or specifically developed in this study, forming the basis for mapping its *SCS* capacity using Equation (1).

3.2. Net Primary Production (NPP)

The net primary production (*NPP*) of agroecosystems is the difference between the carbon fixed by photosynthesis and the carbon released by autotrophic respiration (R_a) in an ecosystem during a convenient timeframe [45], hence representing the assimilated carbon, i.e., the carbon that is available to feed the first heterotrophic level in such an ecosystem [46]. The *NPP* of agroecosystems can be estimated by means of several methods: (i) from inventories of biomass production, both harvestable and non-harvestable, (ii) by using validated models, both empirical and process-based, which simulate the build-up of crop biomass in both reproductive and vegetative organs, and (iii) by estimations based on the remote sensing of NPP-related properties [47].

In this work, the MODIS NPP was used to characterize the spatial variation of the *NPP*, whose calculation was described in detail in Running et al. [48]. The MODIS NPP algorithm provides annual continuous *NPP* estimates at 1 km resolution based on a model that considers the biophysics of photosynthesis and autotrophic respiration and the vegetation feedback to the climate. Specifically, a simple light-use efficiency model is at the core of the algorithm, requiring daily inputs of incoming photosynthetically active radiation (PAR), the minimum temperature over 24 h periods, and a daytime average vapour-pressure deficit. The necessary estimation of R_a is based on leaf area index (LAI) and temperature data.

The MODIS NPP algorithm is a robust methodology. However, in the validations it has undergone throughout different biomes and land uses, including cropland,

it has been shown to smooth differences of *NPP*, hence overestimating it where it is low and underestimating it where it is high [49]. Therefore, in this work, the MODIS NPP was corrected by comparing it with the actual *NPP* obtained from statistics of agricultural yields.

Specifically, the MODIS NPP images of the Valencian Community for the five years 2017–2021 were retrieved. Concurrently, statistics of agricultural yields were obtained for the same years [50–54]. Since these statistics are available on a provincial basis, the MODIS NPP data were averaged per land use, year, and province. In addition, appropriate dry matter coefficients (DM_j), harvest indices (HI_j), and carbon mass fractions in the harvested biomass ($w_{C,j}$) for each j crop were also retrieved from de Paz et al. [55] and Guzmán et al. [56], thus allowing the actual *NPP* of each land use, year, and province ($NPP_{l\text{-}u,y,p}$) to be calculated with Equation (4).

$$NPP_{l\text{-}u,y,p} = \frac{1}{S_{l\text{-}u,y,p}} \sum_{j=1}^{N} \frac{DM_j w_{C,j}}{HI_j} S_{l\text{-}u,y,p,j} Y_{f,l\text{-}u,y,p,j} \quad (4)$$

In Equation (4) $Y_{f,l\text{-}u,y,p,j}$ is the fresh yield and $S_{l\text{-}u,y,p,j}$ is the extent of crop j in the land use l-u, year y and province p, and $S_{l\text{-}u,y,p}$ is the total surface of the land use l-u in the year y and province p. Then, simple linear regression (SLR) was tried to estimate the actual *NPP* from the MODIS NPP, and the model thus obtained was next applied to assess the actual *NPP* in each pixel of the MODIS NPP map.

3.3. Harvest Index (k_1 Coefficient)

The harvest index (*HI*) in lieu of k_1 (Equation (3)) was mapped by first assigning an average *HI* to each land use (Table 1). Next, the assigned harvest indices were spatially allocated by using the geographical delimitations of the different land uses in the land-use map [44]. For citrus, the *HI* of mature orchards was estimated from data obtained for Valencian plantations by Quiñones et al. [57]. For the composite land uses, i.e., (i) herbaceous and vegetables and (ii) woody non-citrus, the land use *HI* was estimated as a crop-extent weighted mean in the Valencian Community using the *HI* data in de Paz et al. [55] and Guzmán et al. [56] and the crop expanses in agricultural statistics [50–54]. For olive trees, the *HI* was taken from Villalobos et al. [58]. For rice, it was taken from Bueno et al. [59]. Then, for vineyards, the *HI* was taken from a study carried out in Murcia, which is an area nearby, similar to the Valencian Community [60].

Table 1. Harvest Indices (HIs) assigned to the different land uses in the IGN (2016) map [44].

Land Use	Harvest Index (HI)	Reference
Citrus	0.33	Quiñones et al. [57]
Herbaceous, vegetables	0.53	This work
Olive	0.55	Villalobos et al. [58]
Pasture	0.19	This work
Rice	0.50	Bueno et al. [59]
Vineyard	0.51	Mota et al. [60]
Woody non-citrus	0.38	This work

Finally, for pasture, the *HI* was estimated as the ratio of the annual grazed pasture to the annual pasture yield. To assess the annual grazed pasture, it was considered (i) that the pasture is only grazed by the livestock, (ii) that the livestock only grazes on pasture, and (iii) that the livestock is composed of sheep and goats, which constitute most of the animal stock in the Valencian Community. Therefore, for this *HI* assessment to be made, the population of sheep and goats per livestock function in the Valencian Community [50–54]

were multiplied by rough estimates of calorie intake per each one (Table 2) and finally divided by a calorie-to-grass-weight conversion coefficient of 4.3 kcal g^{-1}. To estimate the annual pasture yield, the actual *NPP* obtained (Section 4.1) was multiplied by the pasture extent.

Table 2. Estimated calorie intake requirements of sheep and goats.

Livestock Function	Calorie Intake/kcal day^{-1}
Growing	3500
Adult maintenance	1900
Pregnancy	2750
Lactation	4000

Next, the assigned HIs per land use were spatially allocated by using the geographical delimitations of the different land uses [44]. This way, an *HI* map was developed from the land-use map.

3.4. k_2 Coefficient

In the Janzen et al. [18] model, the k_2 coefficient is a parameter representing the proportion of *NPP* that persists in the soil after five years, and is assigned a constant value of 0.15. In the adaptation of the Janzen model to the Valencian Community, the k_2 parameter was treated as a variable defined as

$$k_2 = 0.15^{abcd} \quad (5)$$

where deviations from the global average value of 0.15 are related to (i) soil temperature deviations from the global mean (T = 14.9 °C), (ii) soil water content (SWC) deviations relative to the interval of $\theta_{FC} - x\,(\theta_{FC} - \theta_{PWP})$ to θ_{FC} (x = 0.444), (iii) differences in soil management compared to bare soil conditions and (iv) deviations in *NPP* composition from the global average. These effects were quantified using response functions for temperature (a), SWC (b) and soil management (c) from the RothC model [37], along with a function for *NPP* composition (d) (Appendices A.1–A.3) and then regionalized (Appendix A.4). However, consistent with the conventional management baseline adopted in this study, and to preserve the simplicity of the Janzen model, parameters c and d were set to their defaults of 1. This assumes, respectively, bare soil conditions (c = 1) [37] and no deviation of *NPP* composition from the global average (d = 1).

3.5. k_3 Coefficient

In the Janzen et al. [18] model, the k_3 coefficient is a parameter representing the annual mineralization rate of SOC, and is assigned a constant value of 0.002. In the adaptation of the Janzen model to the Valencian Community, the k_3 coefficient was also treated as variable. Consequently, k_3 was spatially modelled as dependent on the same rate-modifying factors due to soil temperature (a), SWC (b), soil management (c) and SOC composition (d), and taking the same assumptions regarding c and d indicated above for k_2, albeit through a slightly different functional formulation (Appendix A.1):

$$k_3 = 1 - 0.998^{abcd} \quad (6)$$

3.6. Soil Organic-Carbon Stock

A database of soil sites from the study area was compiled by integrating soil information from 34 partial research surveys conducted between 1983 and 2018. Only sites with available data for at least one surface soil layer or horizon were retained. This resulted in

1338 sites with measurements of w_{SOC} and mass fraction of coarse fragments (w_{CF}), and 415 sites with bulk density (ρ_b) data (Table 3).

Table 3. Statistical summary of the soil organic-carbon mass fraction on a dry-matter basis (w_{SOC}), the bulk density (ρ_b) and the coarse-fragment (Ø > 2 mm) mass fraction (w_{CF}) in the topsoil for the database of soil sites.

Statistic	w_{SOC} (%)	ρ_b (g/cm^3)	w_{CF} (%)
Count	1338	415	1338
Minimum	0.15	0.69	0.0
Maximum	5.68	1.78	79.9
Mean	1.54	1.32	12.9
Standard Deviation	1.09	0.15	23.1

The 0–30 cm depth interval is the one recommended as the minimum for SOC assessment in agricultural lands, because this is where most SOC changes usually occur [61]. However, according to the database, the soil-depth intervals that had been sampled at each site were not uniform, because at least two criteria had been used for sampling. These criteria were (i) to split the soil depth according to horizon identification objectives, or (ii) to split the soil depth according to predetermined intervals, depending on the specific objectives of each survey. Therefore, the information on w_{SOC}, ρ_b and w_{CF} for the 0–30 cm depth range was estimated before the geostatistical analysis was performed.

Specifically, for ρ_b and w_{CF}, weighted averages were calculated from the soil layers that partially or totally included the 0–30 cm interval by using the layer thickness as weighting factor. However, for w_{SOC}, the fact that SOC exponentially decreases as depth increases from a maximum at the surface was taken advantage of [62]. Therefore, the average w_{SOC} in the 0-d_B layer ($\overline{w}_{SOC,B}$), with d_B = 30 cm, was estimated from the average w_{SOC} in the 0-d_A layer ($\overline{w}_{SOC,A}$), where d_A corresponds to another depth, preferentially the shallowest available.

$$\overline{w}_{SOC,B} = \frac{d_A(e^{-\delta d_B} - 1)}{d_B(e^{-\delta d_A} - 1)}\overline{w}_{SOC,A} \quad (7)$$

In Equation (7), δ is the logarithmic rate at which the w_{SOC} decreases with depth. The δ parameter was computed from the w_{SOC} against depth data from the same soil site if information from at least two soil layers was available. Otherwise, if only information from one layer was available, δ was calculated from the average w_{SOC} decrease with depth in the whole database.

The extension of the point information to the entire study area was performed by using the following geostatistics approach. First, the experimental semi-variograms for w_{SOC} and w_{CF} were fitted with spherical models and the ρ_b with a Gaussian one, due to the fewer sample points in this case (Figure 2). Then, ordinary kriging was used for the spatial interpolation based on the semi-variograms previously fitted.

Then, the SOC stock was assessed by using map algebra in which the maps of w_{SOC}, ρ_b and w_{CF} were combined according to the following equation.

$$SOC_{stock} = 100\, w_{SOC}\, \rho_b\, (1 - w_{CF})\, d \quad (8)$$

where SOC_{stock} is the SOC stock in Mg ha^{-1}, w_{SOC} is in g g^{-1}, ρ_b in g cm^{-3}, w_{CF} in g g^{-1}, and d is the soil depth in cm, i.e., 30 cm in this work, as previously stated.

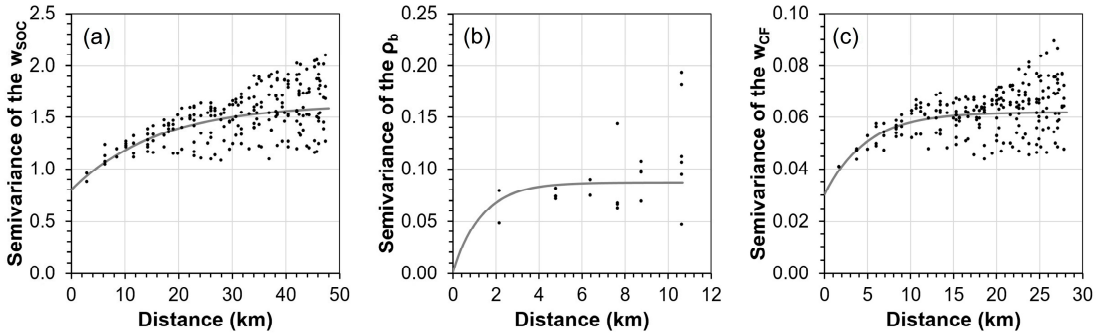

Figure 2. Semi-variograms obtained for the soil organic-matter mass fraction (**a**), the bulk density (**b**) and the coarse-fragment mass fraction (**c**).

3.7. Spatial Processing of the Information

Data processing was conducted using the Geographical Information System (GIS) ArcGIS 9.3 (ESRI; Redlands, CA, USA), following the workflow in Figure 3. Spatial analysis techniques were applied to delineate agricultural areas, distinguishing them from other land uses, and to further subdivide these areas into homogeneous zones to which specific values of intermediate variables—*NPP*, k_1, k_2, k_3 and *SOC*—and, ultimately, the *SCS* capacity, could be assigned. Built-in GIS geostatistical tools were used to interpolate point-based soil property data for mapping purposes. Finally, map algebra was applied to combine the different spatial layers according to Equation (1) and to derive the *SCS* capacity.

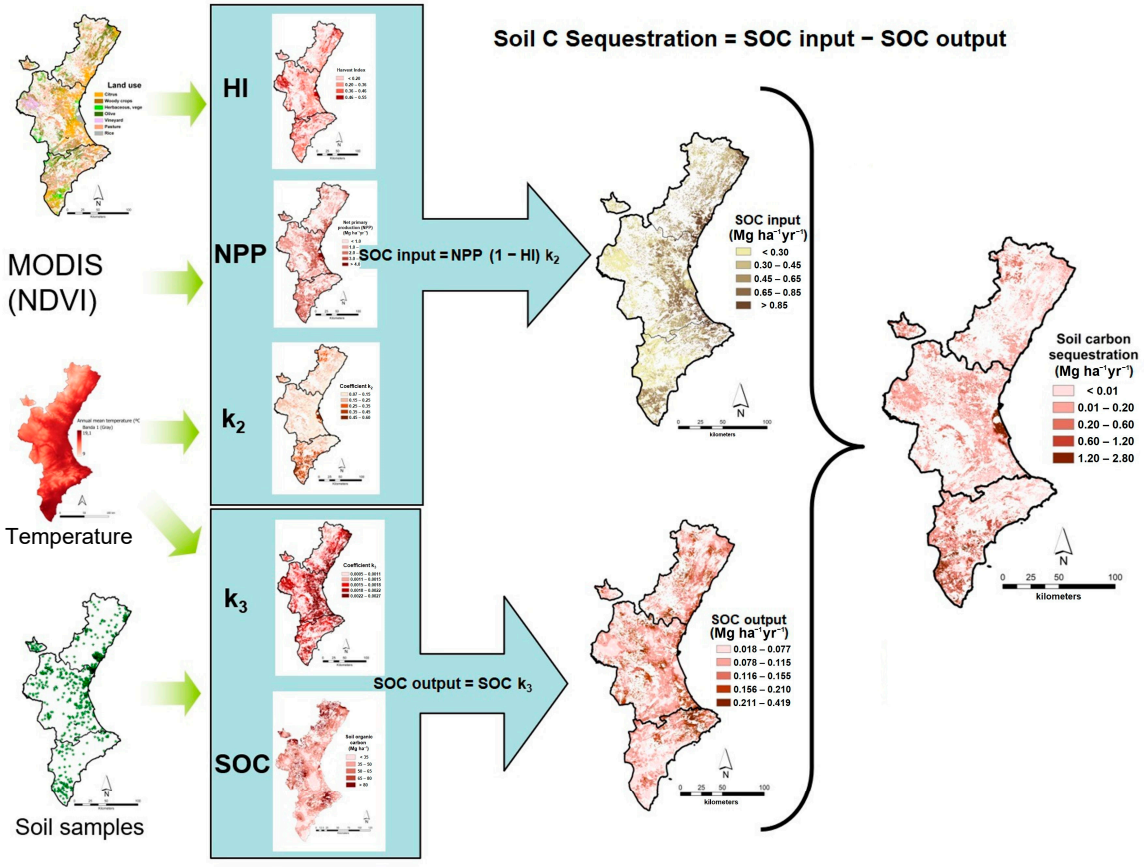

Figure 3. Workflow followed to apply the Janzen et al. [18] model by using geostatistics and map algebra and to derive the spatial distribution of the soil carbon sequestration (*SCS*) capacity across the agricultural lands of the Valencian Community as a function of the net primary production (*NPP*), the soil organic-carbon (SOC) stock and the translocation and transformation coefficients (k_1, k_2 and k_3).

4. Results

4.1. Net Primary Production

Agricultural yield statistics could only be assessed for the following land uses: herbaceous and vegetables, woody non-citrus, citrus, vineyard, olive, and rice; therefore, actual *NPP* could only be obtained and compared to MODIS NPP for these. The comparison, as shown in Figure 4 and Table 4, reveals that, within each land use, MODIS NPP exhibits higher mean and variance than actual *NPP*. The comparison also reveals that the land use explains a remarkable amount of the variance of both. However, the land use explains more variance of the actual *NPP* than of the MODIS *NPP*. In this regard, as the land use changes, both actual and MODIS *NPP* increase. This is in accordance with expectations. However, within each land use, as actual *NPP* increases MODIS *NPP* decreases, which is contrary to expectations.

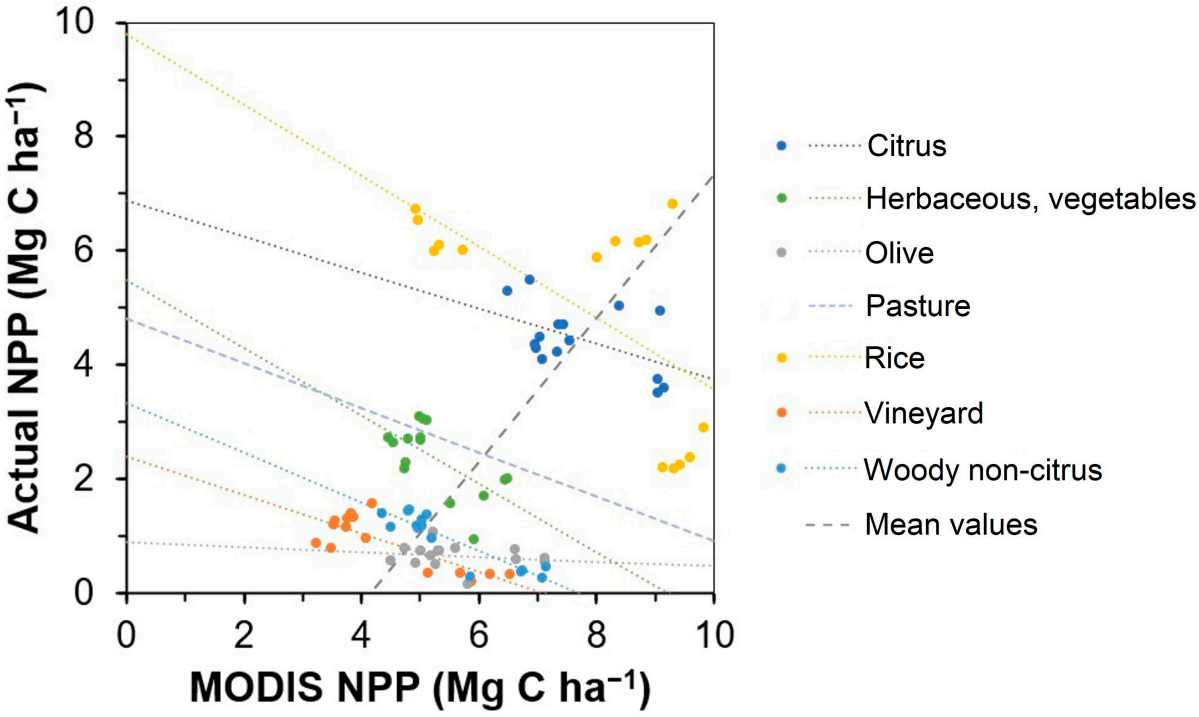

Figure 4. Annual average provincial actual net primary production (*NPP*) versus annual average provincial MODIS-derived *NPP* arranged according to land use in the Valencian Community during 2017–2021. Lines show the simple linear regressions (SLR) of actual against MODIS *NPP* for each land use except pasture, for which the line was estimated by considering the mean slope of all the other land uses and the SLR between mean actual and MODIS *NPP* across all land uses (Mean values).

Therefore, according to the linear dependence that was observed between actual NPP and MODIS NPP within each land use, a different SLR was tried for each one, thereby obtaining the regression coefficients shown in Table 4. For the land uses for which no actual *NPP* data were available, i.e., pasture, the coefficients of the SLR between actual and MODIS NPP were estimated following another approach.

For pasture, the slope of the regression between actual *NPP* and MODIS-derived *NPP* was set equal to the mean slope obtained across the n cropland land uses. The intercept was subsequently calculated using this slope, together with the mean actual *NPP* across the n cropland land uses ($\overline{NPP}_{\text{a,pasture}}$) and the mean MODIS NPP for pasture ($\overline{NPP}_{\text{MODIS,pasture}}$):

$$slope_{\text{pasture}} = \frac{\sum_{i=1}^{n} b_i}{n} \quad (9)$$

$$intercept_{\text{pasture}} = \frac{\sum_{i=1}^{n} \overline{NPP}_{a,i}}{n} - \frac{\sum_{i=1}^{n} b_i}{n} \overline{NPP}_{\text{MODIS,pasture}} \quad (10)$$

Using the SLRs (Table 4), the actual *NPP* was calculated from MODIS *NPP* at the pixel level, producing a spatially distributed *NPP* map (Figure 5). In summary, mean *NPP* by land-use type ranged from 0.64 Mg C ha^{-1} yr^{-1} for olive groves to 6.43 Mg C ha^{-1} yr^{-1} for rice, with citrus ranking second at 4.50 Mg C ha^{-1} yr^{-1}, and a mean of 2.43 Mg C ha^{-1} yr^{-1} over the total land extent (Table 5). In terms of total *NPP*, it ranged from 0.06 Tg C yr^{-1} for olive to 1.02 Tg C yr^{-1} for pasture, with citrus following closely at 0.91 Tg C yr^{-1}, and a grand total of 2.70 Tg C yr^{-1} (Table 5).

Table 4. Descriptive statistics of actual and MODIS *NPP* and of the simple linear regression (SLR) of the former against the latter.

Land Use	NPP (Mg C ha^{-1})				SLR of Actual Against MODIS NPP			Actual NPP †
	Actual		MODIS					
	Mean	Std. Dev.	Mean	Std. Dev.	Slope	Intercept	R^2	
Citrus	4.45	0.59	7.72	0.95	−0.313 *	6.87	0.26	Meas.
Herbaceous, vegetables	2.35	0.62	5.26	0.67	−0.596 **	5.49	0.41	Meas.
Olive	0.64	0.20	5.63	0.85	−0.041 *	0.88	0.32	Meas.
Pasture	2.43	0.58	6.10	0.97	−0.391	4.81	–	Estim.
Rice	4.96	1.91	7.78	1.92	−0.622 **	9.80	0.39	Meas.
Vineyard	0.89	0.47	4.45	1.11	−0.340 **	2.40	0.65	Meas.
Woody non-citrus	0.95	0.46	5.49	0.96	−0.432 **	3.32	0.81	Meas.

* Non-significantly different from zero at the 95% confidence level; ** significantly different from zero at the 95% confidence level; † Estim.: estimated; Meas.: measured.

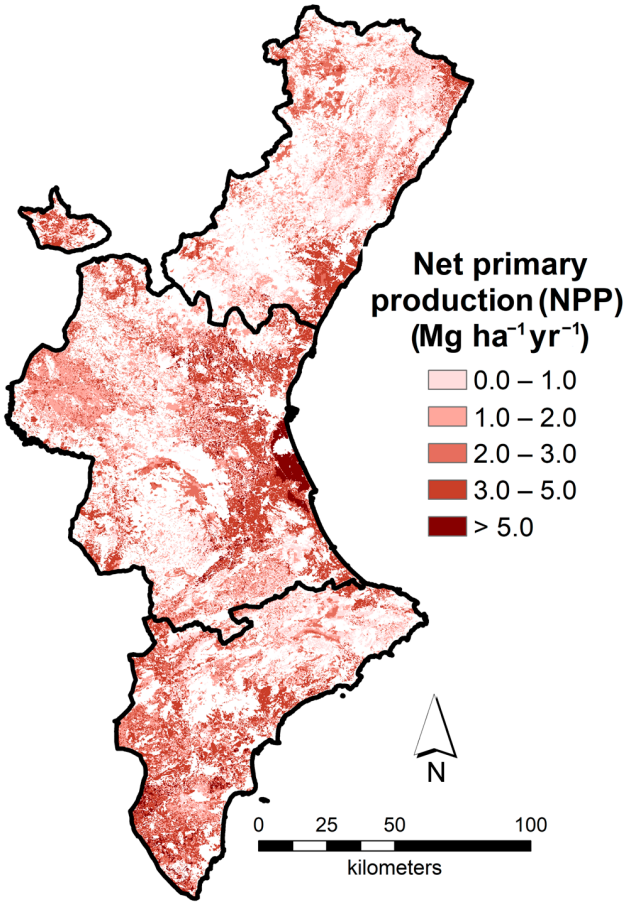

Figure 5. Distribution map of the 2017–2021 average Net Primary Production (*NPP*) across the agricultural lands of the Valencian Community.

Table 5. Extent, net primary production (*NPP*), soil organic-carbon (SOC) stock and soil carbon-sequestration (*SCS*) capacity, both in the topsoil (0–30 cm depth), as a function of the land use.

Land Use	Extent (ha)	NPP		SOC Stock		SCS Capacity	
		Mg C ha^{-1} yr^{-1}	Tg C yr^{-1}	Mg C ha^{-1}	Tg C	Mg C ha^{-1} yr^{-1}	Tg C yr^{-1}
Citrus	201,924	4.50	0.91	53.8	10.9	0.365	0.0736
Herbaceous, vegetables	130,172	2.46	0.32	62.5	8.1	0.189	0.0245
Olive	87,916	0.64	0.06	66.0	5.8	−0.041	−0.0036
Pasture	419,144	2.44	1.02	72.6	30.4	0.356	0.1491
Rice	16,956	6.43	0.11	76.7	1.3	1.308	0.0222
Vineyard	83,020	1.17	0.10	49.3	4.1	0.033	0.0027
Woody non-citrus	174,372	1.07	0.19	65.9	11.5	0.048	0.0084

4.2. Harvest Indices (k_1 Coefficient)

The HI map of the Valencian Community was derived from the land-use map using the HI values assigned in Table 1 (Figure 6). HI values ranged from 0.19 for pasture to 0.55 for olive, with a mean HI of 0.34 across the study area.

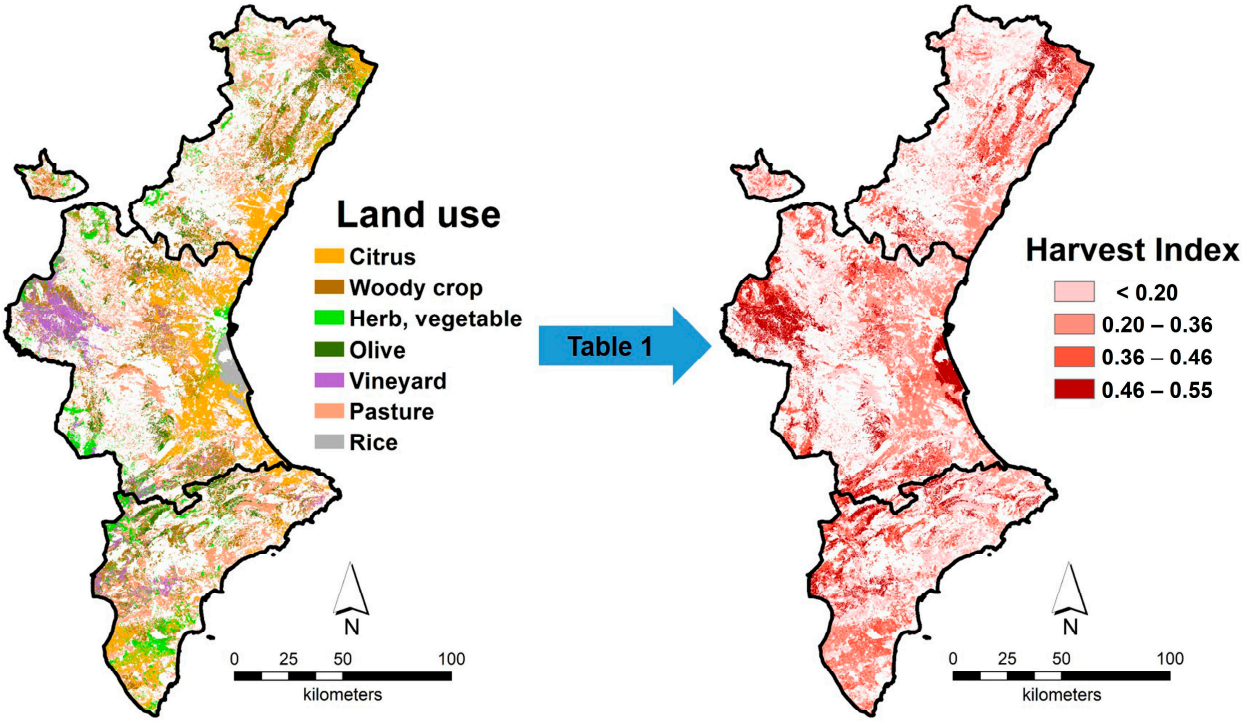

Figure 6. Distribution map of the Harvest Index (HI) across the agricultural lands of the Valencian Community as obtained from the land-use map by using the HI values in Table 1.

4.3. k_2 and k_3 Coefficients

As illustrated in Figure 7, the modeled k_2 coefficient exhibits considerable spatial variability, which runs from 0.16 for citrus to 0.42 for rice, with a mean of 0.21 across the extent of the study area (Table 6).

Similarly to k_2, the modelled k_3 coefficient also exhibits considerable spatial variability (Figure 7), which runs from 0.0012 for rice to 0.0022 for citrus, with a mean of 0.0018 over all the study area (Table 6).

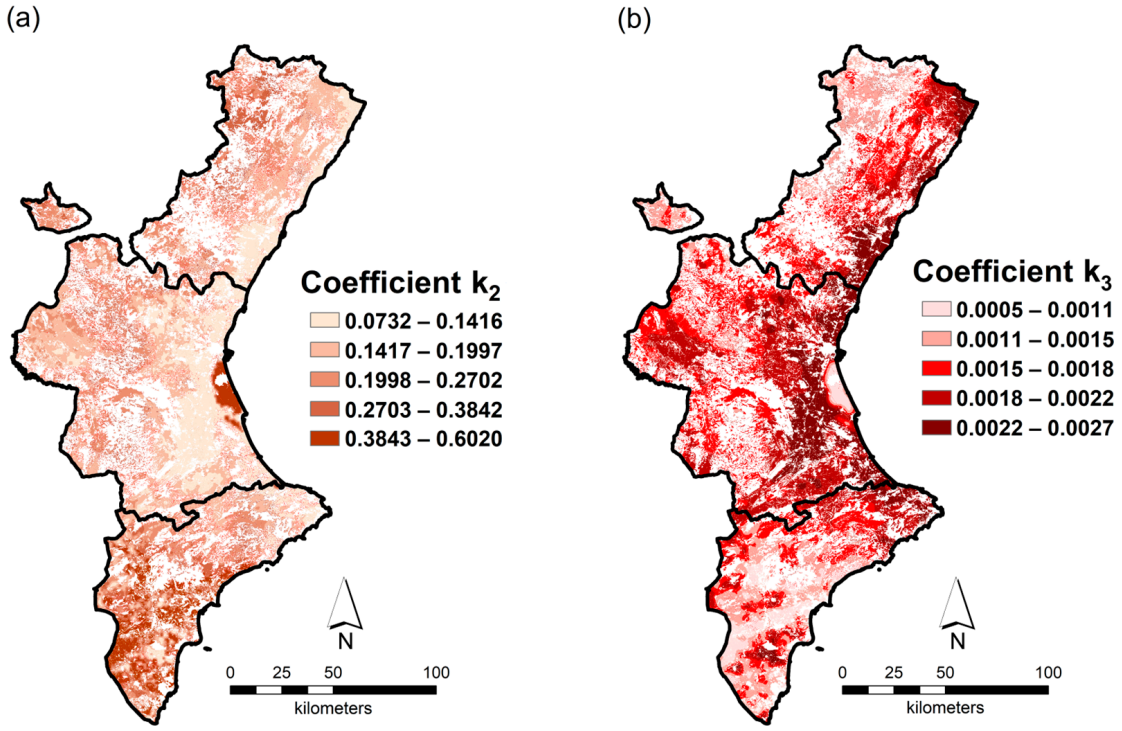

Figure 7. Distribution map of coefficient k_2 (**a**) and coefficient k_3 (**b**) across the agricultural lands of the Valencian Community.

Table 6. Average values of the coefficients k_2 and k_3 as a function of the land use.

Land Use	Extent (ha)	Coefficient k_2	Coefficient k_3
Citrus	201,924	0.156	0.00217
Herbaceous, vegetables	130,172	0.208	0.00178
Olive	87,916	0.200	0.00176
Pasture	419,144	0.235	0.00165
Rice	16,956	0.422	0.00119
Vineyard	83,020	0.185	0.00184
Woody non-citrus	174,372	0.207	0.00174

4.4. Soil Organic-Carbon Stock

The spatial estimations of the topsoil data from which the SOC stock is calculated, i.e., w_{SOC}, ρ_b and w_{CF}, were compared to LUCAS-topsoil measured or estimated w_{SOC}, ρ_b and w_{CF} values [6] as shown in Figure 8. This comparison is not intended to be a validation, but it is convenient because of the benchmark the LUCAS data constitutes for many soil studies in Europe.

For w_{SOC}, the individual estimations appreciably disagree, featuring a Root Mean Square Error (RMSE) of 0.90%, which may be a consequence of the different dates in which the soil points gathered in this work and in the LUCAS campaigns were sampled. However, on average, the estimations of w_{SOC} in this work are consistent with the LUCAS w_{SOC}, as the mean difference at the 95% confidence level of 0.03 ± 0.30% reveals. Regarding ρ_b, the RMSE is 0.29 g cm^{-3} and the mean difference between this work's estimation and LUCAS measurements is 0.18 ± 0.15 g cm^{-3}, which is different from zero at the 95%, but not at the 99% confidence level. Finally, for w_{CF}, the RMSE is 13.2%, but the mean difference between this work's estimations and LUCAS measurements is 0 ± 10%, which is not significatively different from zero at the 95% confidence level.

Therefore, it can be accepted that the w_{SOC}, ρ_b and w_{CF} values from the soil data points gathered in this work are reliable enough to base the SOC stock estimations on them.

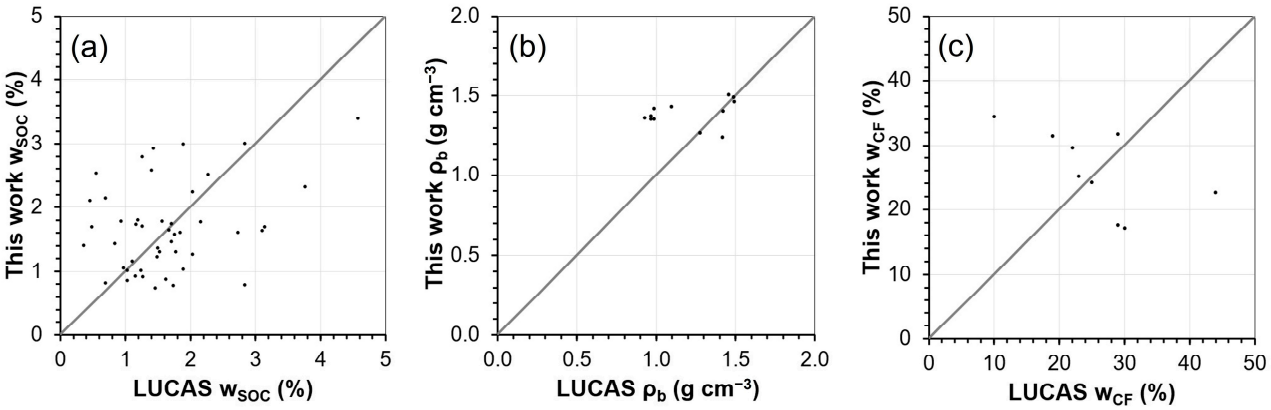

Figure 8. Spatially estimated values in this work for the soil organic-carbon mass fraction (**a**), bulk density (**b**) and the coarse-fragment mass fraction (**c**) against LUCAS measured or estimated values.

Therefore, according to these estimations, the SOC stock in the topsoil (0–30 cm depth) of Valencian agricultural lands was mapped (Figure 9). In summary, it ranges from 49.3 Mg C ha^{-1} for vineyards to 72.6 Mg ha^{-1} for pastures, with a land-extent mean of 64.8 Mg C ha^{-1} for the entire study area, which gives rise to a total of 72.1 Tg C (Table 5).

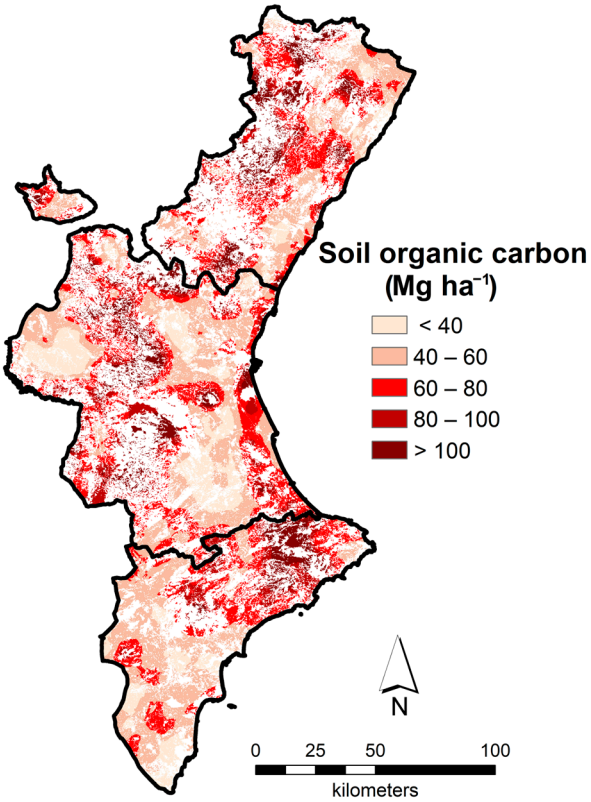

Figure 9. Distribution map of the Soil Organic Carbon stock in the topsoil (0–30 cm depth) across the agricultural lands of the Valencian Community.

4.5. Soil Carbon-Sequestration Capacity

Although the *NPP* of the crops from the Valencian Community lies between 0.64 and 6.43 Mg C ha^{-1} yr^{-1}, with a mean of 2.43 Mg C ha^{-1} yr^{-1} and a total of 2.70 Tg C yr^{-1} (Figure 5; Table 5), the *SCS* capacity of the agricultural lands is remarkably below. Specifically, the *SCS* capacity ranges from −0.04 for olive groves to 1.31 Mg C ha^{-1} yr^{-1} for rice paddies, with a mean of 0.25 Mg C ha^{-1} yr^{-1} for the whole study area, which gives rise to a total of 0.28 Tg C yr^{-1} for Valencian agriculture (Figure 10; Table 5).

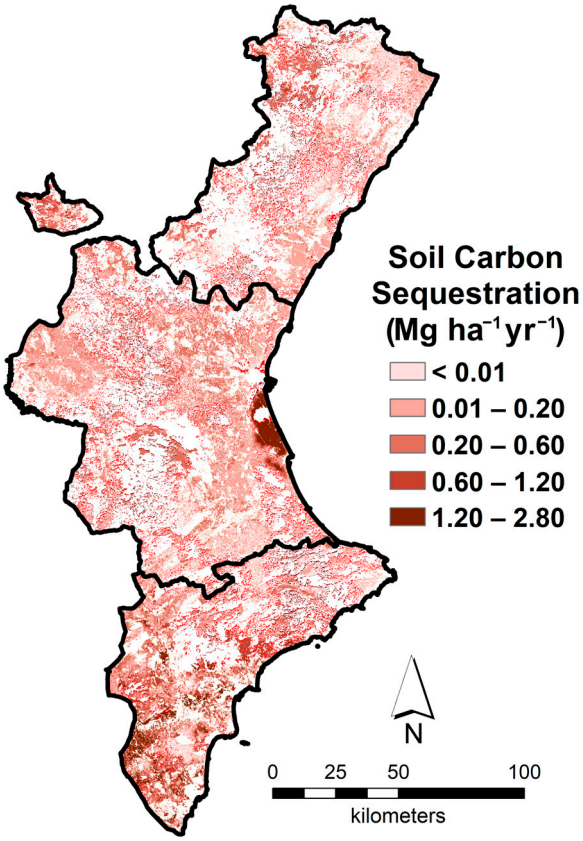

Figure 10. Distribution map of the 2017–2021 average Soil Carbon Sequestration capacity in the topsoil (0–30 cm depth) across the agricultural lands of the Valencian Community.

5. Discussion

5.1. Net Primary Production

The MODIS-derived *NPP* is between 36 and 95% lower than the actual *NPP*. The validation of the MODIS NPP algorithm over other agricultural areas has shown a similar trend of *NPP* underestimation. Specifically, Turner et al. [49] found that the MODIS algorithm underestimated the actual *NPP* of a temperate-climate corn and soybean field by 21%.

Rice shows the strongest agreement between MODIS-derived *NPP* and observed *NPP* in the Valencian Community, with an underestimation of only 36%. This bias is comparable to the previously reported underestimations of 21% for corn and soybean. Notably, rice is the crop in the Valencian Community most similar to corn and soybean. Like these crops, rice is extensively cultivated, and provides a homogeneous soil cover. Moreover, rice is a single-crop land use in this study, which further enhances spatial homogeneity across rice-growing areas. In contrast, *NPP* for the other land uses in the study area is highly underestimated. Unlike rice, these land uses do not provide homogeneous soil cover, due to the presence of bare-soil alleys between plant rows. In addition, several of these land uses, such as vegetables, woody non-citrus crops, and even citrus, are considered multi-crop in this work, therefore leading to further reduced soil-cover homogeneity within their dominant areas.

Consequently, the tendency of the MODIS-derived *NPP* to be biased toward lower values is likely attributable, among other factors, to inhomogeneity in soil cover within and among fields and its effect on the estimation of the gross primary production (*GPP*), which underpins the MODIS *NPP* estimates. *GPP* is computed as the product of the maximum light-use efficiency for carbon fixation (ε) and the photosynthetically active

radiation (*PAR*) that is absorbed by plant canopies, the latter being derived from MODIS reflectance measurements [63]. Consequently, issues in the representativeness of ε and in reflectance-based absorbed *PAR* estimates arising from surface inhomogeneous covering may propagate into biases in *GPP* and, ultimately, in *NPP* [49,63].

Remarkably, however, MODIS-derived and observed *NPP* exhibited an apparent linear relationship independently, for each land use, with the coefficient of determination (R^2) ranging from 0.26 for citrus to 0.81 for woody crops. Although the slope of the SLR was significantly different from zero for only four of the six land uses, particularly those with R^2 over 0.5 (Table 4), the SLRs were used to correct the MODIS underestimation of *NPP* at the pixel level, thereby producing the values that were used for producing the *NPP* map of the Valencian Community.

According to the *NPP* map (Figure 5), the agricultural lands to the north and east of the study area are the most productive, whereas the agricultural lands to the south and west are the least. Water availability, from either rainfall or irrigation, is arguably the most important factor that determines plant productivity [64,65]. In the Valencian Community, the aridity, in general, increases from north to south [66], whereas irrigation dominates the central coastal, eastern and southern parts of the area, and rain-fed cropping prevails in the inland western and northern parts [67].

Therefore, the water availability for agriculture seems to explain a good deal of the geographical distribution of the agricultural *NPP*. Specifically, olive groves, fruit trees and vineyards exhibit the lowest *NPP*, with values of 0.64, 1.07, and 1.17 Mg ha^{-1} (Table 5), largely attributable to water scarcity. In contrast, rice and citrus show the highest *NPP*, with 6.43 and 4.50 Mg ha^{-1}, respectively (Table 5), reflecting much greater water availability. Between both *NPP* extremes, vegetables and pasture exhibit a similar *NPP*, of 2.44 and 2.46 Mg ha^{-1}, respectively.

Olive and grapevine are two crops that have been traditionally rain-fed managed and, though they are nowadays being converted to irrigation in Spain, water supplies are still scarce, thereby limiting their productivity [68,69]. Specifically, less than 20% of the olive-growing area in the Valencian Community receives irrigation [54]. These rainfed-to-irrigation transitional characteristics of olive and grapevine are shared by the almond, which accounts for 64% of the cropping area classified as fruit tree in the Valencian Community [54]. After almond, carob, almost entirely non-irrigated, represents 12% of the fruit-tree area [54].

In addition to water scarcity, crop management may also deliberately decrease the *NPP*. In particular, 91% of the vineyard area in the Valencian Community is devoted to winemaking [54], which is characterized by prioritizing quality over yield. Specifically, for achieving certain must features as a means to obtain desirable wine-quality traits, the vines are managed to constrain both their vegetative and reproductive growth by means of leaf and shoot removals [70], as well as cluster thinning operations [71,72], which keeps their *NPP* well below potential.

At the other *NPP* extreme, there is rice and citrus. Interestingly, cereals like wheat, corn, and rice, along with sugarcane, present the highest biological production among crops, due to their photosynthetic efficiency, high planting density and nitrogen utilization [73,74] and, therefore, it is not surprising that rice, as the most important cereal in the Valencian Community, stands out as the crop with the highest *NPP*. Regarding citrus, they are woody crops like olive and grapevine. However, contrary to the case of these crops, citruses are managed to maximize their productivity by applying irrigation and fertilization schedules that, in general, satisfactorily fulfil their water and nutrient requirements all the year round.

The total *NPP* of the Valencian agroecosystems during 2017–2021 amounted to 2.70 Tg C yr^{-1}. This figure can be compared with the agricultural greenhouse gas (GHG)

emissions of 1.03 Tg CO_2-eq yr^{-1}, i.e., 0.28 Tg C-eq yr^{-1}, which occurred in the same area and time span from processes classified as manure management (36%), non-conservative soil management (30%), enteric fermentation (23%), rice cultivation, burning of agricultural residues, land-use changes and the use of synthetic fertilizers [75]. Therefore, it can be estimated that the Valencian agriculture featured a carbon footprint of −2.42 Tg C yr^{-1} as of 2017–2021.

5.2. Harvest Indices (k_1 Coefficient)

The estimated carbon footprint of −2.42 Tg C yr^{-1} for agriculture in the Valencian Community underscores the significant role agriculture may play in the current climate crisis. However, effective climate change mitigation requires that assimilated carbon does not return to the atmosphere for at least 100 years [19,20]. This requirement contrasts with the brief half-life of assimilated carbon: in harvested biomass it is rapidly consumed and largely returned to the atmosphere within weeks to months, whereas in non-harvested biomass it persists from several months to about one or two years, in the case of herbaceous crops and vegetables, and from one year to a few decades, in the most favorable case of woody crops.

Specifically, the fraction of plant biomass that is not exported from the agricultural fields and contributes to the *NPP* inputs into the soil is given by the difference $1 - HI$. This fraction ranges from 0.45 to 0.81, with a mean value of 0.66 in the study area. Pasture presents the highest $1 - HI$ value, with 0.81. This figure, along with the intermediate *NPP* of pasture and its large expanse, makes this land use the one that contributes the most to the *NPP* inputs into the soil in the study area, with 0.83 Tg C yr^{-1}, specifically 45% of the Valencian agriculture potential for generating *NPP* inputs into the soil. Following pasture, citrus feature the second highest non-exported *NPP* values, with 0.67 (Table 1). Consequently, since citrus present also the second highest *NPP*, it contributes 0.61 Tg C yr^{-1}, i.e., 33% of the Valencian agriculture potential for generating *NPP* inputs into the soil in the form of rhizodepositions, fallen leaves and pruning wood. Similarly, other woody crops show non-exported *NPP* values comparable to citrus (0.62). However, for most other land uses, less than half of the NPP is left within the agricultural system (Table 1), fundamentally limiting the *SCS* capacity of agriculture in the study area.

In particular, for vegetable crops, the $1 - HI$ is often low, as most of the plant biomass is harvested, leaving few residues in the field, and with onion (0.03), carrot (0.31), and the green-leaved ones, e.g., lettuce (0.38) and spinach (0.39), standing out [55]. However, there are other vegetables that are important producers of crop residues, e.g., artichoke (0.78) and cauliflower (0.75) [55], thus making the expanse-weighted average $1 - HI$ of horticulture only somewhat below that of the vineyards (0.47).

Besides boasting intermediate $1 - HI$ values, vegetables also present an *NPP* between that of grapevines and citrus, so both facts mean that horticulture lies halfway between both extremes as a contributor of *NPP* inputs to the soil, in the study area. Interestingly, horticultural crops might rank higher in *NPP* inputs because they are the ones typically receiving more manure applications. Therefore, the organic carbon input represented by *IOMI* in Equation (2) is generally non-negligible for vegetable systems. However, under the conventional management baseline adopted here, *IOMI* is neglected, and the term was set to zero.

If, conversely, *IOMI* were assumed to be non-zero, the estimated *NPP* inputs to the soil, and consequently the estimated *SOC input* and *SCS* capacity of vegetable systems, would increase. Moreover, owing to its higher proportion of stabilized organic fractions, manure typically mineralizes more slowly than other SOC inputs, e.g., crop residues, and, therefore, this characteristic would enhance its contribution to SCS [76–78]. Accordingly,

excluding *IOMI* from the model has resulted in an underestimation of SCS, especially in horticultural systems where organic amendments are more prevalent.

5.3. k_2 and k_3 Coefficients

The variable mineralization rate of the *SOC input* due to its composition would be reflected by variations in k_2. Nevertheless, by assuming $d = 1$ in Equation (5) this investigation did not address potential variability in k_2 related to the *SOC input* composition, focusing only on the effects of soil temperature and moisture. Because these factors in the Valencian Community differ markedly from their global averages, k_2 deviates substantially from the global mean of 0.15 [18], with more than 74% of the study area exhibiting higher values (Figure 7). The highest ones, exceeding 0.40, are predominantly found in two contrasting environments: (i) rice paddies, where anaerobic conditions due to high SWC minimize microbial decomposition of crop residues, and (ii) the drier southern part of the region, where low SWC constrains decomposition, thereby promoting higher soil retention of crop residues.

The k_3 coefficient exhibits an antiparallel trend relative to k_2 (Figure 7), because of their opposite definitions (Equations (5) and (6)). The k_3 changes according to several factors such as climate, soil texture and tillage [79]. However, by assuming $c = 1$ in Equation (6) according to the conventional management baseline adopted in this work, only the influence of soil temperature and moisture has been considered. Accordingly, our results show a clear spatial pattern in k_3, depending on both factors (Figure 7), with (i) rice paddies exhibiting the lowest values (<0.0011), because anoxic conditions strongly reduce microbial activity and thus carbon mineralization, and (ii) coastal areas, with the exception of paddy areas, presenting the highest k_3 (>0.0022), indicating enhanced mineralization rates under their favorable temperature and SWC conditions.

5.4. Soil Organic-Carbon Stock

The spatial predictions of the topsoil variables used to calculate SOC stock, i.e., w_{SOC}, ρ_b, and w_{CF}, were, on average, consistent with the corresponding LUCAS topsoil measurements (Figure 8), although the fitting precision was limited. In contrast, w_{SOC} predictions derived from the Organic Carbon content in the TOPsoils dataset (OCTOP) showed systematic disagreement with the LUCAS observations in the Valencian Community, resulting in a marked underestimation [80]. Therefore, this analysis improves previous modelling efforts and strengthens confidence in the pixel-level estimates of SOC stocks that have been carried out in this study.

The highest SOC stocks in the Valencian Community are located in three areas: the northwest, center and southeast (Figure 9). These three areas feature dry–subhumid climate conditions and lower temperatures, in contrast to the semi-arid and warmer characteristics of the rest of the study area [66], and such climate conditions may explain how SOC lasts longer, something which eventually shows up in higher SOC stocks. Conversely, the lower SOC stocks are located to the south of the area, where the climate is warmer and drier.

Higher temperatures generally enhance SOC decomposition [81], whereas climatic dryness tends to favor SOC preservation by constraining soil biological activity [82]. However, the high-intensity rainfall events characteristic of the Mediterranean climate can substantially accelerate SOM respiration beyond the enhancing effects of intermediate SWC [83]. This response may be largely attributed to rewetting effects, which accelerate SOC mineralization and can override the SOC gains accumulated during preceding dry periods [82,84,85]. In addition, increasing rainfall intensity enhances SOC losses through water erosion [86]. Water erosion may therefore represent a significant factor of SOC loss in the Valencian Community, particularly in southern areas, where SOC stocks are lower,

because of their steep relief and semi-arid-to-arid conditions. In these areas, very limited vegetation cover on the alleys between plant rows leaves soils remarkably exposed to raindrop impact and compaction from agricultural traffic, resulting in low infiltration capacity and high susceptibility to runoff.

Regarding the SOC stock in the topsoil under the different land uses, vineyard feature the lowest, with 49.3 Mg C ha^{-1} (Table 5), which is surprisingly higher than the estimate made for French vineyards, which is roughly 32 Mg C ha^{-1} [87,88]. The SOC stock for citrus follows, with 53.8 Mg C ha^{-1} (Table 5), which is like that of Chinese citrus orchards [89]. The SOC stock in vegetable systems is 62.4 Mg C ha^{-1}, which is higher than French croplands, which feature 56.4 Mg ha^{-1} [87]. Surprisingly, the SOC stock for olive groves is quite high, i.e., 66.0 Mg ha^{-1} (Table 5), which is like the values found for olive groves cropped under the same hot-summer Mediterranean climate in southern Italy [90].

The high SOC stock featured by olive groves is probably because olive trees are usually grown in agroforestry areas, which are aimed at not only producing olives, but, importantly, at raising swine, thus favoring the development of spontaneous plants that contribute a lot of plant debris to the soil [91]. However, under the conventional management approach adopted in this study, only one plant, i.e., the crop, or an average one in the case of vegetables and fruit-trees, treated separately, has been considered.

5.5. Soil Carbon-Sequestration Capacity

On average, the Valencian agriculture would be able to assimilate 2.43 Mg C ha^{-1} yr^{-1} and sequester in the soil 0.25 Mg C ha^{-1} yr^{-1}. This *SCS* capacity compares well with the results of Follet [92], who assessed an *SCS* capacity of between 0.1 and 0.6 Mg C ha^{-1} yr^{-1} for US croplands. Since the SOC stock in the topsoil from the study area is 72.1 Tg C, the whole *SCS* capacity of 0.28 Tg C yr^{-1} of the Valencian agroecosystems leads to an annual increase of 3.8 per mille, thus almost matching the objective of 4 per mille that was raised in the COP21 agreement in Paris [24].

If both the *NPP* and the *SCS* capacity are compared by land use (Table 5), rice is not only the highest in the former (6.43 Mg C ha^{-1} yr^{-1}), but also in the latter (1.31 Mg C ha^{-1} yr^{-1}). Conversely, olives, grapevines and fruit trees sequester very little carbon in the soil (−0.041, 0.033 and 0.048 Mg C ha^{-1} yr^{-1}), which is in accordance with the low *NPP* of 0.64, 1.17 and 1.07 Mg C ha^{-1} yr^{-1} which they feature, respectively, as well as their relatively low $1 - HI$, which means that roots, pruning wood and fallen leaves contribute very little to the *SOC input* under these land uses. Moreover, this contribution would more favorably occur in cases where these crop residues were incorporated into soils. However, this is a management practice not very widespread in, particularly, the vineyards of the study area, because of concerns about the role dead-wood debris may play as shelter for fungal plant pathogens, specifically behaving as an inoculum source for grapevine trunk diseases from one year to the next [93,94]. However, the low *SCS* that vineyards feature could be increased if RSM practices were implemented, such as the use of cover crops or the importation of organic amendments [95,96], provided these have been conveniently sanitized and decontaminated.

The *SCS* of 0.28 Tg C yr^{-1} of the agricultural land of the Valencian Community amounts to only 10% of its *NPP*. Moreover, according to the agricultural greenhouse gas (GHG) emissions of 0.28 Tg C-eq yr^{-1}, which were contributed in the same area during 2017–2021 [75], the *SCS* of the Valencian agroecosystems would have made up just 100% of these. In this way, Valencian agriculture would offset its emissions and become carbon neutral, primarily because of pasture (0.15 Tg C yr^{-1}) and citrus (0.07 Tg C yr^{-1}), due to their large extent and moderate SCS capacity. However, nothing would be left to compensate for emissions from past agricultural activity or from other anthropogenic

sectors. Therefore, though the agricultural *SCS* is considered a strategy for climate change mitigation, these results suggest that, by itself, the *SCS* of agroecosystems cannot fix the present climate crisis, as already addressed [24,97,98].

The only way in which Valencian agriculture may contribute to offset the GHG emissions from the past and other anthropogenic sectors in the same region, and therefore help mitigate climate change, is by growing from the conventional baseline of 0.28 Tg C yr^{-1}. In this regard, the widespread deployment of RSM practices, particularly in areas identified in this study as having the most favorable conditions, emerges as the most effective strategy. By increasing SOM, these practices not only contribute to climate change mitigation, but also enhance soil health by reinforcing soil ecological functions, thereby improving land adaptation to climate change [99].

In particular, under the arid-to-dry sub-humid climate featured in the Valencian Community, the soil health enhancement the SOM increase brings about might boost agricultural yields [100] and harvest quality [101], thus decisively supporting Valencian agriculture in its adaptation to climate change. However, more research is needed to support this hypothesis of mutually reinforcing effects due to the implementation of RSM, especially for woody crops.

Remarkably, the deployment of RSM must be system specific, as shown in this work. In irrigated systems, the focus should be on enhancing *SCS* through active management practices, chiefly the regular incorporation of crop residues into the soil and the use of cover crops, either sown or spontaneous, because without groundcover the agroecosystem *NPP* is below its maximum [102,103], while additionally bare soil conditions promote SOC decomposition (c = 1 for bare soil and c = 0.6 otherwise in Equations (5) and (6)). In particular, citrus is the most promising land use for *SCS* in the Valencian Community, because of the high *NPP* it boasts in combination with a low SOC stock (Table 5), and then the low harvest index (0.33), and the large expanse of land it covers (Table 5). Therefore, the implementation of RSM practices to increase the *SCS* under citrus, such as the use of cover crops, the recirculation of organic matters and reduced tillage could enhance the *SCS*.

In rainfed systems, where increasing *NPP* is inherently challenging due to water scarcity, the primary objective should be soil conservation and the preservation of existing SOC stocks. This can be achieved by minimizing soil disturbance; for instance, by adopting minimum-till practices. Moreover, the abuse of tillage operations negatively impacts soil fauna and fungi survival rates [104,105] and boosts soil aeration remarkably [106], thus accelerating the mineralization of both the ephemeral and lingering SOC pools, which would show up in the increase of the k_2 and k_3 coefficients.

Furthermore, conventional tillage also renders the soil highly erodible, resulting in SOC losses because of topsoil water erosion [107,108]. The effect of water erosion on *SCS* would enter Equation (1) as an SOC output, i.e., a subtrahend. Therefore, excluding water erosion from the present analysis to preserve the simplicity of Janzen's model may have led to *SCS* overestimation. Nevertheless, this *SCS* overestimation could be, at least in part, counterbalanced by the *SCS* underestimation caused by disregarding cover crops, both seeded and spontaneous, as well as organic-matter recirculation to croplands as SOC inputs.

6. Conclusions

The Janzen's simple soil-carbon sequestration (SCS) model has been adapted and applied at regional scale within a GIS framework, using the calibrated *NPP* map, the SOC stock map from a geostatistical analysis of layered-soil point data, and the land-use map combined with crop-specific harvest indices for the study area, together with spatially distributed estimates of *NPP* and SOC decay-rate coefficients. Using this approach, the

spatial distribution of SCS capacity under conventional management across a representative semi-arid Mediterranean agricultural region has been explored, showing that it ranges from -0.04 to 1.31 Mg C ha^{-1} yr^{-1}.

The geographic distribution of *SCS* is primarily controlled by water availability, either from rainfall or irrigation, because of its control over the *NPP*, SOC and *NPP* and SOC decay-rate coefficients. In total, under the assumption of conventional crop and soil management, the agroecosystems from the study area may assimilate 2.70 Tg C yr^{-1}, i.e., the *NPP*, and sequester 0.28 Tg C yr^{-1} in the soil, i.e., barely 10% of the *NPP*, led by pasture and citrus with 0.15 and 0.07 Tg C yr^{-1}, respectively, due to their large extent and moderate *SCS* capacity. This total *SCS* would have nearly met the 4-per-mille objective and accounted for 100% of the greenhouse gas (GHG) emissions from agriculture in the study area, which were 0.28 Tg C-eq yr^{-1} during the five-year period 2017–2021. Therefore, the total SCS that has been estimated just offsets the agricultural GHG emissions.

This result suggests that under continued conventional crop and soil management, without enhancing the agricultural carbon sink, the *SCS* of agriculture in the study area is insufficient to offset GHG emissions from past agricultural activity or from other anthropogenic sectors and, therefore, the objectives of the "carbon farming" strategies will not be met. Nevertheless, fortunately, the *SCS* can only increase from the 0.28 Tg C yr^{-1} conventional baseline, hence overcoming the 4-per-mille objective, if the following regenerative soil management (RSM) practices are implemented: (i) the use of cover crops to increase the agroecosystem *NPP*, and decrease SOC loss due to mineralization and soil water erosion; (ii) the application of organic amendments, to recirculate as much *NPP* as possible to agroecosystems; (iii) and reduced tillage, to decrease the *NPP* and SOC mineralization rates and SOC losses because of water erosion.

Importantly, such an *SCS* increase may strengthen the soil health of agriculture in the study area, with likely consequences of enhancement of crop yields and harvest quality. The geographic distribution of *SCS* in the study area, as revealed in this work, can adequately support decision-makers in planning the implementation of RSM practices aimed at increasing *SCS*. However, which RSM practices are more adequate and how they should be applied to obtain the most *SCS*, as well as to enhance produce yield and quality, must be researched in more depth.

Author Contributions: Conceptualization, J.M.d.P., D.J.I. and F.V.; methodology, J.M.d.P., S.M. and F.V.; software, J.M.d.P. and F.V.; validation, F.V.; formal analysis, E.P., F.V.; investigation, E.P., S.M. and F.V.; resources, D.J.I. and S.M.; data curation, E.P., S.M. and F.V.; writing—original draft preparation, J.M.d.P. and F.V.; writing—review and editing, F.V.; visualization, J.M.d.P. and F.V.; supervision, J.M.d.P.; project administration, J.M.d.P.; funding acquisition, J.M.d.P. All authors have read and agreed to the published version of the manuscript.

Funding: This research was funded by the SOSTESABIO project (IVIA-GVA 52203C). The predoctoral contract of S.M. was supported by a "Marisa Badenes" fellowship (MB2025_22) entitled "Adecuación del sistema agrario de la Comunitat Valenciana a la agricultura del carbono" funded by the Instituto Valenciano de Investigaciones Agrarias (IVIA) through budget allocation G.542G00.19001, fund FS21000019.

Data Availability Statement: The data presented in this study are available on request from the corresponding author.

Acknowledgments: The authors thank the Spanish State Meteorological Agency (AEMET) for providing the climate data used in this study.

Conflicts of Interest: The authors declare no conflicts of interest.

Abbreviations

The following abbreviations are used in this manuscript:

GIS	Geographical Information System
HI	Harvest Index
IOMI	Imported Organic Matter Index
LUCAS	Land Use/Cover Area frame Survey Soil
MODIS	Moderate Resolution Imaging Spectroradiometer
NPP	Net Primary Production
RSM	Regenerative Soil Management
SCS	Soil Carbon Sequestration
SOC	Soil Organic Carbon

Appendix A

Appendix A.1. Coefficients of the Janzen et al. [18] Model for a One-Year Time Span Under Variable Non-Standard Soil Temperature and Moisture

The residual net primary production (*RNPP*) and the soil organic carbon (*SOC*) that remain in the soil t years after time $t = 0$ can be calculated with, respectively, Equations (A1) and (A2), which consider that they both decay according to first-order kinetics:

$$RNPP = RNPP_0 e^{-k_{\mathrm{RNPP}} t} \quad \text{(A1)}$$

$$SOC = SOC_0 e^{-k_{\mathrm{SOC}} t} \quad \text{(A2)}$$

In Equation (A1), $RNPP_0$ is the residual net primary production at time $t = 0$ ($RNPP_0 = (1 - HI)\ NPP$), and k_{RNPP} is the decomposition first-order kinetics rate coefficient of the residual net primary production. In Equation (A2), in parallel to Equation (A1), SOC_0 is the soil organic carbon at time $t = 0$, and k_{SOC} is the decomposition first-order kinetics rate coefficient of the soil organic carbon.

The decomposition rate of organic carbon depends on the composition of the organic matter, weather conditions, and how it is managed. Therefore, the decomposition rate coefficient of organic carbon can be expressed as the product of several factors, each accounting for one of these influences [37]. Accordingly, we can write the following equations as applied to the RNPP and SOC, respectively:

$$k_{RNPP} = a\ b\ c\ d\ k_{\mathrm{RNPP,std}} \quad \text{(A3)}$$

$$k_{SOC} = a\ b\ c\ d\ k_{\mathrm{SOC,std}} \quad \text{(A4)}$$

where a, b, c and d are modifying factors that account for, respectively, soil temperature, soil water content, organic carbon management and composition of the organic matter, and $k_{\mathrm{RNPP,std}}$ and $k_{\mathrm{SOC,std}}$ represent the decomposition rate coefficients under standard conditions of soil temperature (T), soil water content (θ), organic composition and conventional crop and soil management, for which $a = 1$, $b = 1$, $d = 1$ and $c = 1$, respectively.

In the Janzen et al. [18] model, the decomposition rate coefficients for RNPP and SOC differ from the k_{RNPP} and k_{SOC} definitions. Specifically, in the Janzen et al. [18] model, the coefficient for RNPP decomposition, denoted as k_2, was defined as the fraction of the RNPP remaining after five years under standard conditions of T, θ and biomass composition so $a = 1$, $b = 1$ and $d = 1$, and conventional crop and soil management so $c = 1$, while the coefficient for *SOC* decomposition, denoted as k_3, was defined as the fraction of *SOC*

decomposed in one year, also under standard conditions of T, θ and soil organic matter composition so $a = 1$, $b = 1$ and $d = 1$, and conventional soil management so $c = 1$. Therefore,

$$k_2 = \frac{RNPP_1}{RNPP_0} = e^{-k_{\mathrm{RNPP,std}}} \tag{A5}$$

$$k_3 = 1 - \frac{SOC_1}{SOC_0} = 1 - e^{-k_{\mathrm{SOC,std}}} \tag{A6}$$

By using Equations (A1)–(A4), the fraction of RNPP remaining after one year, on the one hand, and the fraction of SOC decomposed after one year, on the other hand, under non-standard and non-conventional management conditions, i.e., conditions so that $a \neq 1$, $b \neq 1$, $d \neq 1$ and $c \neq 1$, can be obtained:

$$k_{2,\mathrm{non-std}} = \frac{RNPP_1}{RNPP_0} = e^{-abcdk_{\mathrm{RNPP,std}}} \tag{A7}$$

$$k_{3,\mathrm{non-std}} = 1 - \frac{SOC_1}{SOC_0} = 1 - e^{-abcdk_{\mathrm{SOC,std}}} \tag{A8}$$

Therefore, if the value of $k_{\mathrm{RNPP,std}}$ is isolated from both Equations (A5) and (A7) and equaled, and if the same is done with the value of $k_{\mathrm{SOC,std}}$ in Equations (A6) and (A8), the decomposition coefficients in the Janzen et al. [18] model for a one-year time span and under non-standard T, θ, organic carbon management and organic matter composition ($k_{2,\text{non-std}}$ and $k_{3,\text{non-std}}$) can be expressed based on the k_2 and k_3 as originally defined for standard conditions and conventional management:

$$k_{2,\mathrm{non-std}} = k_2^{abcd} \tag{A9}$$

$$k_{3,\mathrm{non-std}} = 1 - (1 - k_3)^{abcd} \tag{A10}$$

Appendix A.2. Decomposition Rate Modifying Temperature Factor a Regarding the Global Mean Temperature

The following expression can be assumed for the decomposition rate modifying temperature factor a [37]:

$$a = \frac{\alpha}{1 + e^{\beta/(T+\gamma)}} \tag{A11}$$

where T is in °C and α, β and γ are constants that take values of, respectively, 47.9, 106 and 18.3, so that the standard temperature at which $a = 1$ is the annual mean temperature for Rothamsted, England [37], which is 9.25 °C.

However, the decomposition rate coefficients k_2 and k_3 in the Janzen et al. [18] model take the global mean temperature as standard, not Rothamsted's.

The decomposition rate modifying temperature factor a in Equation (A11) can be defined as the ratio of the decomposition rate coefficient at whichever temperature T to the decomposition rate factor at the standard temperature, i.e., Rothamsted's (T_{R}), by means of the following equation:

$$\frac{k_T}{k_{T_{\mathrm{R}}}} = \frac{\alpha}{1 + e^{\beta/(T+\gamma)}} \tag{A12}$$

Therefore, at another temperature, e.g., global mean temperature (T_{G}), the decomposition rate modifying temperature factor is the following:

$$\frac{k_{T_{\mathrm{G}}}}{k_{T_{\mathrm{R}}}} = \frac{\alpha}{1 + e^{\beta/(T_{\mathrm{G}}+\gamma)}} \tag{A13}$$

By dividing Equation (A12) by Equation (A13), the decomposition rate modifying temperature factor a at temperature T with regards to temperature T_G is obtained:

$$\frac{k_T}{k_{T_G}} = \frac{1 + e^{\beta/(T_G+\gamma)}}{1 + e^{\beta/(T+\gamma)}} \tag{A14}$$

If we define α_G as

$$\alpha_G = 1 + e^{\beta/(T_G+\gamma)} \tag{A15}$$

and calculate it for the global mean temperature T_G = 14.9 °C, we obtain α_G = 25.4, which is the value that should be used instead of 47.9 to calculate the decomposition rate modifying temperature factor a regarding the global mean temperature, with the following equation in which β and γ present the same values of 106 and 18.3, respectively:

$$a_G = \frac{\alpha_G}{1 + e^{\beta/(T+\gamma)}} \tag{A16}$$

Appendix A.3. Decomposition Rate Modifying Soil Moisture Factor b

The decomposition rate modifying soil water content (SWC) factor b was originally defined based on the topsoil moisture deficit (*TSMD*):

$$b = \begin{cases} b_{min} & \text{if } TSMD > TSMD_{max} \\ b_{min} + (b_{max} - b_{min}) \frac{TSMD_{max} - TSMD}{TSMD_{max} - xTSMD_{max}} & \text{if } TSMD \in [x,\ 1]\ TSMD_{max} \\ b_{max} & \text{if } TSMD < x\ TSMD_{max} \end{cases} \tag{A17}$$

where b_{min} and b_{max} are the bottom and top bounds of the b factor: b_{min} = 0.2 and b_{max} = 1.0, 0; $TSMD_{max}$ are the bottom and top bounds of the *TSMD*; and x is a fraction ($0 \leq x \leq 1$) of the *TSMD* range, i.e., from 0 to $TSMD_{max}$, which is taken as being x = 0.444.

The *TSMD* can be defined in terms of the SWC (θ), the SWC at field capacity (θ_{FC}), and the SWC at permanent wilting point (θ_{PWP}), and the $TSMD_{max}$:

$$TSMD = \frac{\theta_{FC} - \theta}{\theta_{FC} - \theta_{PWP}} TSMD_{max} \tag{A18}$$

Then *TSMD* in Equation (A17) can be replaced by its definition according to Equation (A18), and b can be expressed based on the SWC (Figure A1):

$$b = \begin{cases} b_{min} & \text{if } \theta < \theta_{PWP} \\ b_{min} + (b_{max} - b_{min}) \frac{\theta - \theta_{PWP}}{(1-x)(\theta_{FC} - \theta_{PWP})} & \text{if } \theta \in [\theta_{PWP},\ x\ \theta_{PWP} + (1-x)\theta_{FC}\ ] \\ b_{max} & \text{if } \theta > x\ \theta_{PWP} + (1-x)\theta_{FC} \end{cases} \tag{A19}$$

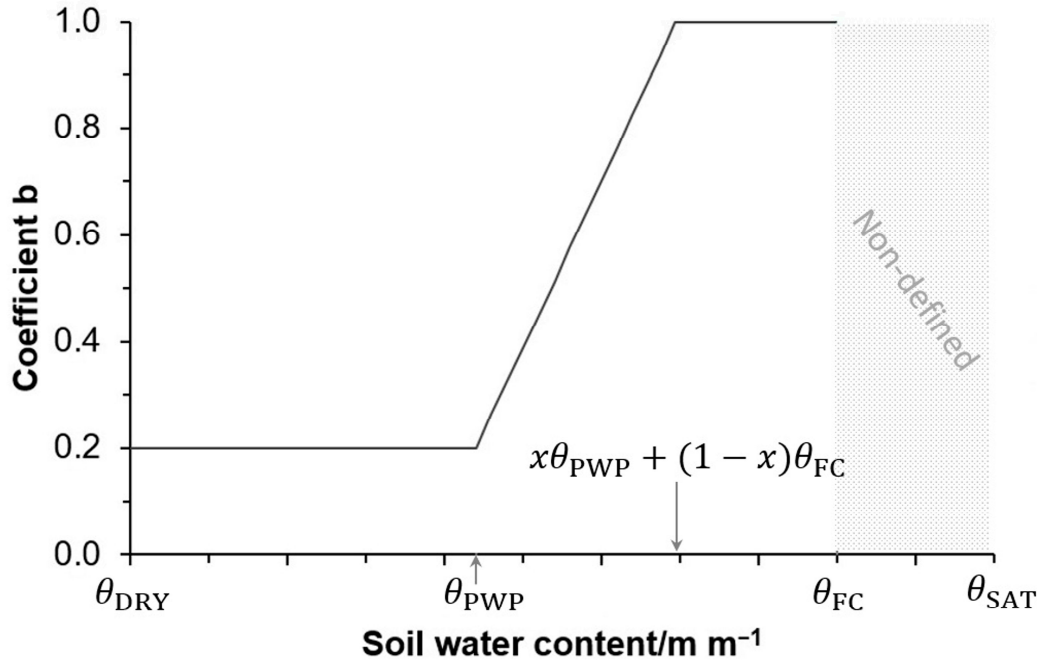

Figure A1. Coefficient b evolution as function of the soil water content (SWC) from dryness (θ_{DRY} = 0) to field capacity (θ_{FC}), passing through permanent wilting point (θ_{PWP}), and the transition to optimum SWC for soil organic-carbon mineralization, which is $x\ \theta_{PWP} + (1 - x)\ \theta_{FC}$ with x = 0.444, according to Coleman et al. [37]. Between θ_{FC} and water saturation (θ_{SAT}), the coefficient b is not defined, which limits the application of this calculation to conditions where SWC is expected to be as much as θ_{FC}.

Appendix A.4. Assessment of the Spatial Distribution of the a and b Coefficients

The coefficients of the Janzen et al. [18] model under variable non-standard temperature (T) and SWC (θ) conditions ($k_{2,\text{non-std}}$ and $k_{3,\text{non-std}}$) were spatially estimated by first assessing the spatial distribution of the coefficients a and b on which they depend (Equations (A9) and (A10)).

To spatially estimate the soil-temperature coefficient a, air temperature (T_{air}) was used as surrogate for soil temperature (T). Consequently, rasterized monthly T_{air} for the 1991–2020 climatological mean was obtained from AEMET [109] and used directly to compute the rasterized monthly a coefficient using Equation (A16). The 12 monthly values were subsequently averaged to derive the annual mean map of the coefficient a throughout the Valencian Community (Figure A2).

To spatially estimate the SWC coefficient b, a spatially distributed soil-water balance was performed. Previously, the SWC at permanent wilting point (θ_{WP}) and at field capacity (θ_{FC}) were spatially generated by geostatistical interpolation of the soil properties required to apply the Mualem–van Genuchten soil-water retention model at pressure heads of −15,000 and −200 cm, respectively. Model parameters were taken from the calibration of Wösten et al. [110] for European soils, and from the resulting SWC the volume occupied by coarse fragments was subtracted.

Next, rasterized monthly cumulative rainfall (R) and Penman–Monteith reference evapotranspiration (ET_0) for the 1991–2020 climatological mean were obtained from AEMET [109]. Crop evapotranspiration for each month i ($ET_{c,i}$) was computed as the product of land-use-specific crop coefficients (K_i, Table A1) and reference evapotranspiration:

$$ET_{c,i} = K_i\ ET_{0,i} \quad \text{(A20)}$$

Annual irrigation rates (I) were also selected, depending on the land use (Table A2), and distributed across months according to the following equation:

$$I_i = \frac{IR_i}{\sum_{i=1}^{12} IR_i} I \tag{A21}$$

where IR_i denotes the irrigation requirement for month i, calculated as the difference between crop evapotranspiration and precipitation for that month. Negative values were set to zero (Equation (A22)).

$$IR_i = \begin{cases} 0 & \text{if } K_{c,i}ET_{c,i} - P_i \leq 0 \\ K_{c,i}ET_{c,i} - P_i & \text{if } K_{c,i}ET_{c,i} - P_i > 0 \end{cases} \tag{A22}$$

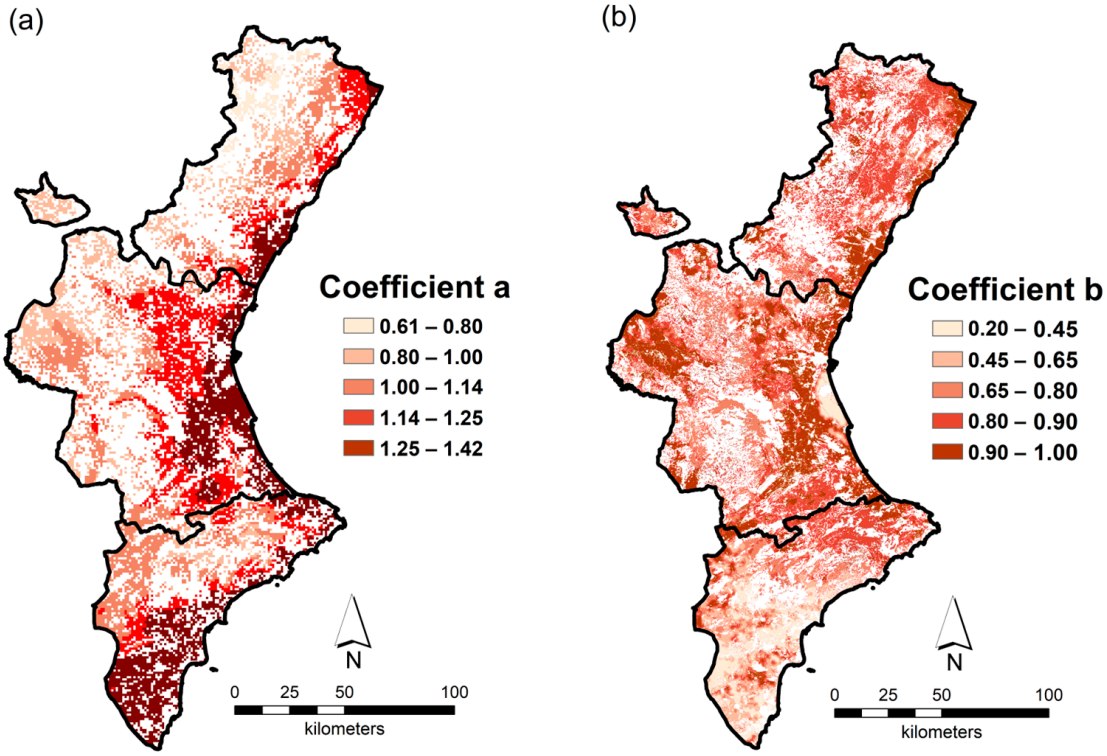

Figure A2. Distribution map of the soil-temperature coefficient a (**a**) and the soil-moisture coefficient b (**b**) throughout the agricultural lands of the Valencian Community. Data from AEMET [109].

Table A1. Monthly crop coefficients (K_i) used to calculate crop evapotranspiration.

Land Use	Jan	Feb	Mar	Apr	May	Jun	Jul	Aug	Sep	Oct	Nov	Dec
Citrus	0.63	0.62	0.63	0.59	0.52	0.59	0.65	0.75	0.70	0.80	0.69	0.60
Herb., veg.	0.46	0.47	0.48	0.48	0.50	0.51	0.51	0.49	0.47	0.46	0.46	0.47
Olive	0.45	0.45	0.59	0.54	0.50	0.50	0.50	0.50	0.50	0.54	0.59	0.45
Pasture	0.46	0.47	0.48	0.48	0.50	0.51	0.51	0.49	0.47	0.46	0.46	0.47
Rice	–	–	–	–	–	–	–	–	–	–	–	–
Vineyard	0.00	0.00	0.00	0.29	0.29	0.33	0.40	0.41	0.42	0.37	0.00	0.00
Woody N. Cit.	0.00	0.05	0.23	0.39	0.53	0.60	0.64	0.69	0.62	0.53	0.19	0.00

Table A2. Annual irrigation rates used for estimating monthly irrigation rates.

Land Use	Irrigation (mm)
Citrus	394
Herbaceous, vegetables	392
Olive	0
Pasture	0
Rice	–
Vineyard	146
Woody non-citrus (almond, carob, pomegranate, persimmon, etc.)	120

The water balance was initialized in September (month 9), which marks the beginning of the hydrological year, by setting the SWC equal to the wilting point ($\theta_9 = \theta_{WP}$). Subsequently, the SWC for the ith month (θ_i) was computed by adding monthly precipitation (P_i) and irrigation (I_i) to the SWC at the end of the previous $(i-1)$th month and subtracting crop evapotranspiration. The resulting θ_i was constrained to lie between θ_{WP} and θ_{FC}: values below θ_{WP} were set to θ_{WP}, and values above θ_{FC} were set to θ_{FC} (Equation (A23)). The water balance was iterated until convergence of θ_9 was achieved.

$$\theta_i = \begin{cases} \theta_{WP} & \text{if } \theta_{i-1} + P_i + I_i - ET_{c,i} < \theta_{WP} \\ \theta_{i-1} + P_i + I_i - ET_{c,i} & \text{if } \theta_{i-1} + P_i + I_i - ET_{c,i} \in [\theta_{WP},\ \theta_{FC}] \\ \theta_{FC} & \text{if } \theta_{i-1} + P_i + I_i - ET_{c,i} > \theta_{FC} \end{cases} \quad \text{(A23)}$$

The rasterized monthly SWC values were used to compute the rasterized monthly b coefficient using Equation (A19).

The water-balance approach combined with the calculation of coefficient b in Appendix A.3 was not applied to rice-land use because paddy fields remain flooded for several months annually and, in all cases in the study area, are characterized by shallow water tables. These features result in paddy soils that are either water-saturated or remain between field capacity and saturation year-round, which are conditions that are not simulated by the water-balance approach in combination with the calculation of coefficient b in Appendix A.3. However, these over field-capacity conditions lead to b coefficient values consistently below unity, with lower values associated with higher soil-water content [111]. Therefore, coefficient b was assigned according to the values found by calibration by Shirato and Yokozawa [111]: $b = 0.2$ during flooded months, $b = 0.6$ during drainage months, and, consequently, $b = 0.4$ during transition months between flooded and drained conditions, following the rice water cycle in the paddy fields around L'Albufera [112], which is the most important rice-cropping area in the Valencian Community (Figure A3).

In both cases—application of the water balance and coefficient b calculation approach in Appendix A.3, and the rice land-use case—the 12 monthly b values were averaged to derive an annual mean map of coefficient b across the Valencian Community. The rasterized parameters representing the mean annual coefficients a and b (Figure A2) were then used to compute the final $k_{2non\text{-}std}$ and $k_{3non\text{-}std}$ maps.

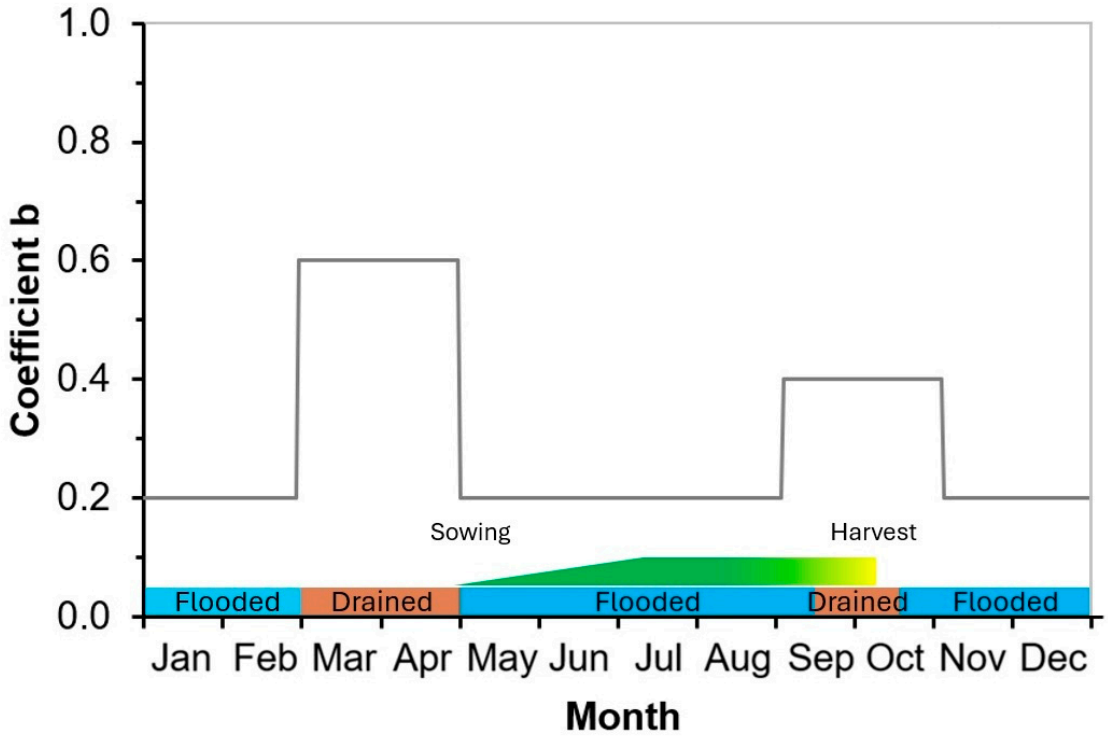

Figure A3. Average monthly values of coefficient *b* assigned to paddy soils based on the water cycle in the paddy fields around L'Albufera (Valencian Community).

References

1. Bai, Z.G.; Dent, D.L.; Olsson, L.; Schaepman, M.E. Proxy global assessment of land degradation. *Soil Use Manag.* **2008**, *24*, 223–234. [CrossRef]
2. Pereira, P.; Bogunovic, I.; Muñoz-Rojas, M.; Brevik, E.C. Soil ecosystem services, sustainability, valuation and management. *Curr. Opin. Environ. Sci. Health* **2018**, *5*, 7–13. [CrossRef]
3. Smith, P.; House, J.I.; Bustamante, M.; Sobocká, J.; Harper, R.; Pan, G.; West, P.C.; Clark, J.M.; Adhya, T.; Rumpel, C.; et al. Global change pressures on soils from land use and management. *Glob. Change Biol.* **2016**, *22*, 1008–1028. [CrossRef]
4. Prăvălie, R. Exploring the multiple land degradation pathways across the planet. *Earth-Sci. Rev.* **2021**, *220*, 103689. [CrossRef]
5. Mueller, L.; Schindler, U.; Mirschel, W.; Graham Shepherd, T.; Ball, B.C.; Helming, K.; Rogasik, J.; Eulenstein, F.; Wiggering, H. Assessing the productivity function of soils: A review. *Agron. Sustain. Dev.* **2010**, *30*, 601–614. [CrossRef]
6. Panagos, P.; Van Liedekerke, M.; Borrelli, P.; Köninger, J.; Ballabio, C.; Orgiazzi, A.; Lugato, E.; Liakos, L.; Hervas, J.; Jones, A.; et al. European Soil Data Centre 2.0: Soil data and knowledge in support of the EU policies. *Eur. J. Soil Sci.* **2022**, *73*, e13315. [CrossRef]
7. Ferreira, C.S.S.; Seifollahi-Aghmiuni, S.; Destouni, G.; Ghajarnia, N.; Kalantari, Z. Soil degradation in the European Mediterranean region: Processes, status and consequences. *Sci. Total Environ.* **2022**, *805*, 150106. [CrossRef] [PubMed]
8. European Commission. *A Farm to Fork Strategy for a Fair, Healthy and Environmentally-Friendly Food System*; Communication from the Commission, COM(2020) 381 Final; European Commission: Brussels, Belgium, 2020. Available online: https://eur-lex.europa.eu/legal-content/EN/TXT/?uri=CELEX:52020DC0381 (accessed on 9 June 2024).
9. European Commission. *Proposal for a Directive of the European Parliament and of the Council on Soil Monitoring and Resilience (Soil Monitoring Law)*; COM(2023) 416 Final; European Commission: Brussels, Belgium, 2023. Available online: https://eur-lex.europa.eu/legal-content/EN/TXT/?uri=COM%3A2023%3A0416%3AFIN (accessed on 9 June 2024).
10. Visconti, F.; López, R.; Olego, M.Á. The health of vineyard soils: Towards a sustainable viticulture. *Horticulturae* **2024**, *10*, 154. [CrossRef]
11. Lal, R. Sequestration of atmospheric CO_2 in global carbon pools. *Energy Environ. Sci.* **2008**, *1*, 86–100. [CrossRef]
12. Martin, J.B. Carbonate minerals in the global carbon cycle. *Chem. Geol.* **2017**, *449*, 58–72. [CrossRef]
13. Aguilera, E.; Guzmán, G.I.; Álvaro-Fuentes, J.; Infante-Amate, J.; García-Ruiz, R.; Carranza-Gallego, G.; Soto, D.; González de Molina, M. A historical perspective on soil organic carbon in Mediterranean cropland (Spain, 1900–2008). *Sci. Total Environ.* **2018**, *621*, 634–648. [CrossRef]

14. Bellamy, P.H.; Loveland, P.J.; Bradley, R.I.; Lark, R.M.; Kirk, G.J.D. Carbon losses from all soils across England and Wales 1978–2003. *Nature* **2005**, *437*, 245–248. [CrossRef]
15. Capriel, P. Trends in organic and nitrogen content in agricultural soils in Bavaria (South Germany) between 1986 and 2007. *Eur. J. Soil Sci.* **2013**, *64*, 445–454. [CrossRef]
16. Heikkinen, J.; Ketoja, E.; Nuutinen, V.; Regina, K. Declining trend of carbon in Finnish cropland soils in 1974–2009. *Glob. Change Biol.* **2013**, *19*, 1456–1469. [CrossRef] [PubMed]
17. Lal, R. Soil carbon sequestration impacts on global climate change and food security. *Science* **2004**, *304*, 1623–1627. [CrossRef]
18. Janzen, H.H.; van Groenigen, K.J.; Powlson, D.S.; Schwinghamer, T.; van Groenigen, J.W. Photosynthetic limits on carbon sequestration in croplands. *Geoderma* **2022**, *416*, 115810. [CrossRef]
19. Stockmann, U.; Adams, M.A.; Crawford, J.W.; Field, D.J.; Henakaarchchi, N.; Jenkins, M.; Minasny, B.; McBratney, A.B.; de Courcelles, V.; Singh, K.; et al. The knowns, known unknowns and unknowns of sequestration of soil organic carbon. *Agric. Ecosyst. Environ.* **2013**, *164*, 80–99. [CrossRef]
20. UNFCCC. *Common Metrics*; United Nations Framework Convention on Climate Change: Bonn, Germany, 2022. Available online: https://unfccc.int/process-and-meetings/transparency-and-reporting/methods-for-climate-change-transparency/common-metrics (accessed on 5 February 2026).
21. Jansson, C.; Faiola, C.; Wingler, A.; Zhu, X.-G.; Kravchenko, A.; de Graaff, M.-A.; Ogden, A.J.; Handakumbura, P.P.; Werner, C.; Beckles, D.M. Crops for carbon farming. *Front. Plant Sci.* **2021**, *12*, 636709. [CrossRef]
22. Lötjönen, S.; Kulovesi, K.; Lång, K.; Ollikainen, M. Offset ratios and temporary contract designs for climate integrity in carbon farming. *Carbon Manag.* **2024**, *15*, 2329593. [CrossRef]
23. Wertebach, T.M.; Hölzel, N.; Kämpf, I.; Yurtaev, A.; Tupitsin, S.; Kiehl, K.; Kamp, J.; Kleinebecker, T. Soil carbon sequestration due to post-Soviet cropland abandonment: Estimates from a large-scale soil organic carbon field inventory. *Glob. Change Biol.* **2017**, *23*, 3729–3741. [CrossRef]
24. Minasny, B.; Malone, B.P.; McBratney, A.B.; Angers, D.A.; Arrouays, D.; Chambers, A.; Chaplot, V.; Chen, Z.S.; Cheng, K.; Das, B.S.; et al. Soil carbon 4 per mille. *Geoderma* **2017**, *292*, 59–86. [CrossRef]
25. Conant, R.T.; Cerri, C.E.; Osborne, B.B.; Paustian, K. Grassland management impacts on soil carbon stocks: A new synthesis. *Ecol. Appl.* **2017**, *27*, 662–668. [CrossRef]
26. Paustian, K.; Lehmann, J.; Ogle, S.; Reay, D.; Robertson, G.P.; Smith, P. Climate-smart soils. *Nature* **2016**, *532*, 49–57. [CrossRef]
27. Paustian, K.; Collier, S.; Baldock, J.; Burgess, R.; Creque, J.; DeLonge, M.; Dungait, J.; Ellert, B.; Frank, S.; Goddard, T.; et al. Quantifying carbon for agricultural soil management: From the current status toward a global soil information system. *Carbon Manag.* **2019**, *10*, 567–587. [CrossRef]
28. FAO. *Global Soil Organic Carbon Sequestration Potential Map—GSOCseq v1.1*; FAO: Rome, Italy, 2022. [CrossRef]
29. Giri, R.K.K.V.; Mandla, V.R. Study and evaluation of carbon sequestration using remote sensing and GIS: A review on various techniques. *Int. J. Civ. Eng. Technol.* **2017**, *8*, 287–300. Available online: https://iaeme.com/Home/issue/IJCIET?Volume=8&Issue=4 (accessed on 15 March 2026).
30. Falloon, P.; Smith, P.; Szabó, J.; Pásztor, L. Comparison of approaches for estimating carbon sequestration at the regional scale. *Soil Use Manag.* **2002**, *18*, 164–174. [CrossRef]
31. Chen, S.; Martin, M.P.; Saby, N.P.A.; Walter, C.; Angers, D.A.; Arrouays, D. Fine resolution map of top- and subsoil carbon sequestration potential in France. *Sci. Total Environ.* **2018**, *630*, 389–400. [CrossRef] [PubMed]
32. Lugato, E.; Bampa, F.; Panagos, P.; Montanarella, L.; Jones, A. Potential carbon sequestration of European arable soils estimated by modelling a comprehensive set of management practices. *Glob. Change Biol.* **2015**, *21*, 3557–3567. [CrossRef]
33. Cole, V.; Cerri, C.; Minami, K.; Mosier, A.; Rosenberg, N.; Sauerbeck, D. Agricultural options for mitigation of greenhouse gas emissions. In *Climate Change 1995: Impacts, Adaptations and Mitigation of Climate Change*; Watson, R.T., Moss, R.H., Zinyowera, M.C., Eds.; Cambridge University Press: Cambridge, UK, 1996; pp. 745–771.
34. Cole, C.V.; Duxbury, J.; Freney, J.; Heinemeyer, O.; Minami, K.; Mosier, A.; Paustian, K.; Rosenberg, N.; Sampson, N.; Sauerbeck, D.; et al. Global estimates of potential mitigation of greenhouse gas emissions by agriculture. *Nutr. Cycl. Agroecosyst.* **1997**, *49*, 221–228. [CrossRef]
35. Smith, P.; Martino, D.; Cai, Z.; Gwary, D.; Janzen, H.; Kumar, P.; McCarl, B.; Ogle, S.; O'Mara, F.; Rice, C.; et al. Greenhouse gas mitigation in agriculture. *Philos. Trans. R. Soc. B* **2008**, *363*, 789–813. [CrossRef]
36. Smith, P. Land use change and soil organic carbon dynamics. *Nutr. Cycl. Agroecosyst.* **2008**, *81*, 169–178. [CrossRef]
37. Coleman, K.; Jenkinson, D.S.; Crocker, G.J.; Grace, P.R.; Klír, J.; Körschens, M.; Poulton, P.R.; Richter, D.D. Simulating trends in soil organic carbon in long-term experiments using RothC-26.3. *Geoderma* **1997**, *81*, 29–44. [CrossRef]
38. Parton, W.J.; Rasmussen, P.E. Long-term effects of crop management in wheat–fallow: CENTURY model simulations. *Soil Sci. Soc. Am. J.* **1994**, *58*, 530–536. [CrossRef]

39. Del Grosso, S.J.; Parton, W.J.; Mosier, A.R.; Hartman, M.D.; Brenner, J.; Ojima, D.S.; Schimel, D.S. Simulated interaction of soil carbon dynamics and nitrogen trace gas fluxes using the DAYCENT model. In *Modeling Carbon and Nitrogen Dynamics for Soil Management*; Shaffer, M.J., Ma, L., Hansen, S., Eds.; Lewis Publishers: Boca Raton, FL, USA, 2001; pp. 303–332.
40. Li, C.S. *User's Guide to the DNDC Model (Version 9.5)*; Institute for the Study of Earth, Oceans, and Space, University of New Hampshire: Durham, NH, USA, 2012.
41. Farina, R.; Marchetti, A.; Francaviglia, R.; Napoli, R.; Di Bene, C. Modeling regional soil C stocks and CO_2 emissions under Mediterranean cropping systems and soil types. *Agric. Ecosyst. Environ.* **2017**, *238*, 128–141. [CrossRef]
42. Visconti, F.; de Paz, J.M. Estimation of the potential CO_2 sequestration and emission capacity of the agricultural soils of the Valencian Community. *Ecosistemas* **2017**, *26*, 91–100. [CrossRef]
43. Riffaldi, R.; Saviozzi, A.; Levi-Minzi, R. Carbon mineralization kinetics as influenced by soil properties. *Biol. Fertil. Soils* **1996**, *22*, 293–298. [CrossRef]
44. IGN. *Sistema de Información Sobre Ocupación del Suelo de España (SIOSE)*; Instituto Geográfico Nacional: Madrid, Spain, 2016. Available online: http://www.siose.es (accessed on 30 April 2024).
45. Schlesinger, W.H. *Biogeochemistry: An Analysis of Global Change*; Academic Press: San Diego, CA, USA, 1997.
46. Lindeman, R.L. The trophic-dynamic aspect of ecology. *Ecology* **1942**, *23*, 399–417. [CrossRef]
47. Ito, A. A historical meta-analysis of global terrestrial net primary productivity: Are estimates converging? *Glob. Change Biol.* **2011**, *17*, 3161–3175. [CrossRef]
48. Running, S.W.; Nemani, R.R.; Heinsch, F.A.; Zhao, M.; Reeves, M.; Hashimoto, H. A continuous satellite-derived measure of global terrestrial primary production. *BioScience* **2004**, *54*, 547–560. [CrossRef]
49. Turner, D.P.; Ritts, W.D.; Cohen, W.B.; Gower, S.T.; Running, S.W.; Zhao, M.; Costa, M.H.; Kirschbaum, A.A.; Ham, J.M.; Saleska, S.R.; et al. Evaluation of MODIS NPP and GPP products across multiple biomes. *Remote Sens. Environ.* **2006**, *102*, 282–292. [CrossRef]
50. MAPA. *Anuario de Estadística 2018*; Ministerio de Agricultura, Pesca y Alimentación: Madrid, Spain, 2018. Available online: https://www.mapa.gob.es (accessed on 1 July 2024).
51. MAPA. *Anuario de Estadística 2019*; Ministerio de Agricultura, Pesca y Alimentación: Madrid, Spain, 2019. Available online: https://www.mapa.gob.es (accessed on 1 July 2024).
52. MAPA. *Anuario de Estadística 2020*; Ministerio de Agricultura, Pesca y Alimentación: Madrid, Spain, 2020. Available online: https://www.mapa.gob.es (accessed on 1 July 2024).
53. MAPA. *Anuario de Estadística 2021*; Ministerio de Agricultura, Pesca y Alimentación: Madrid, Spain, 2021. Available online: https://www.mapa.gob.es (accessed on 1 July 2024).
54. MAPA. *Anuario de Estadística 2022*; Ministerio de Agricultura, Pesca y Alimentación: Madrid, Spain, 2022. Available online: https://www.mapa.gob.es (accessed on 1 July 2024).
55. De Paz, J.M.; Ramos, C.; Visconti, F. Critical nitrogen dilution curve and dry matter production parameters for several Mediterranean vegetables. *Sci. Hortic.* **2022**, *303*, 111194. [CrossRef]
56. Guzmán, G.I.; Aguilera, E.; Soto, D.; Cid, A.; Infante, J.; García, R.; Herrera, A.; Villa, I.; González de Molina, M. Methodology and conversion factors to estimate the net primary productivity of historical and contemporary agroecosystems (I). *Doc. Trab. Soc. Estud. Hist. Agrar.* **2014**, *1407*, 1–52.
57. Quiñones, A.; Martínez-Alcántara, B.; Font, A.; Forner-Giner, M.A.; Legaz, F.; Primo-Millo, E.; Iglesias, D. Allometric models for estimation of carbon fixation in citrus trees. *Agron. J.* **2013**, *105*, 1355–1366. [CrossRef]
58. Villalobos, F.J.; Testi, L.; Hidalgo, J.; Pastor, M.; Orgaz, F. Modelling potential growth and yield of olive (*Olea europaea* L.) canopies. *Eur. J. Agron.* **2006**, *24*, 296–303. [CrossRef]
59. Bueno, S.B.; Lafarge, T. Higher crop performance of rice hybrids than of elite inbreds in the tropics: Hybrids accumulate more biomass during each phenological phase. *Field Crops Res.* **2009**, *112*, 229–239. [CrossRef]
60. Mota, C.; Alcaraz-López, C.; Iglesias, M.; Martínez-Ballesta, M.C.; Carvajal, M. Investigación sobre la absorción de CO_2 por los cultivos más representativos de la región de Murcia. *Hortic. Glob.* **2011**, *294*, 58–63.
61. IPCC. *Land Use, Land-Use Change, and Forestry*; Cambridge University Press: Cambridge, UK, 2000.
62. Mishra, U.; Lal, R.; Slater, B.; Calhoun, F.; Liu, D.; Van Meirvenne, M. Predicting soil organic carbon stock using profile depth distribution functions and ordinary kriging. *Soil Sci. Soc. Am. J.* **2009**, *73*, 614–621. [CrossRef]
63. Xin, Q.; Broich, M.; Suyker, A.; Yu, L.; Gong, P. Multi-scale evaluation of light use efficiency in MODIS gross primary productivity for croplands in the Midwestern United States. *Agric. For. Meteorol.* **2015**, *201*, 111–119. [CrossRef]
64. Kukal, M.S.; Irmak, S. Irrigation-limited yield gaps: Trends and variability in the United States post-1950. *Environ. Res. Commun.* **2019**, *1*, 061005. [CrossRef]
65. Ali, M.M.; Yousef, A.F.; Li, B.; Chen, F. Effect of environmental factors on growth and development of fruits. *Trop. Plant Biol.* **2021**, *14*, 226–238. [CrossRef]

66. De Paz, J.M.; Visconti, F.; Zapata, R.; Sánchez, J. Integration of two simple models in a geographical information system to evaluate salinization risk in irrigated land of the Valencian Community, Spain. *Soil Use Manag.* **2004**, *20*, 333–342. [CrossRef]
67. Romero-González, J.; Tortosa, F. El regadío. In *Atlas Temático de la Comunidad Valenciana*; Morales-Gil, A., Marco-Molina, J.A., Eds.; Levante-EMV: Valencia, Spain, 1991; Volume 2, pp. 501–520.
68. Fernández, J.E.; Diaz-Espejo, A.; Romero, R.; Hernandez-Santana, V.; García, J.M.; Padilla-Díaz, C.M.; Cuevas, M.V. Precision irrigation in olive (*Olea europaea* L.) orchards. In *Water Scarcity and Sustainable Agriculture in Semiarid Environment*; Garcia Tejero, I., Durán Zuazo, V.H., Eds.; Academic Press: London, UK, 2018; pp. 179–217. [CrossRef]
69. García-Escudero, E.; Martínez, J.M. Evolución del cultivo de la vid en España en los últimos cincuenta años. In *Tecnología Hortícola Mediterránea*; Namesny, A., Conesa, C., Martín, L., Papasselt, P., Eds.; SPE3: Valencia, Spain, 2022; pp. 959–986.
70. Smart, R.E.; Robinson, M. *Sunlight into Wine: A Handbook for Winegrape Canopy Management*; Winetitles: Adelaide, Australia, 1991.
71. Guidoni, S.; Ferrandino, A.; Novello, V. Effect of cluster thinning on berry skin anthocyanin composition of *Vitis vinifera* cv. Nebbiolo. *Am. J. Enol. Vitic.* **2002**, *53*, 224–226. [CrossRef]
72. Keller, M.; Mills, L.J.; Wample, R.L.; Spayd, S.E. Cluster thinning effects on three deficit-irrigated *Vitis vinifera* cultivars. *Am. J. Enol. Vitic.* **2005**, *56*, 91–103. [CrossRef]
73. Baffes, J.; Etienne, X. Yield growth patterns of food commodities: Insights and challenges. *PLoS ONE* **2024**, *19*, e0313088. [CrossRef]
74. Qiao, M.; Hong, C.; Jiao, Y.; Hou, S.; Gao, H. Impacts of drought on photosynthesis in major food crops and the related mechanisms of plant responses to drought. *Plants* **2024**, *13*, 1808. [CrossRef]
75. GVA. *Informe del Inventario de Emisiones de GEI. Comunitat Valenciana. Datos 2020*; Generalitat Valenciana: Valencia, Spain, 2022. Available online: https://mediambient.gva.es (accessed on 24 July 2024).
76. Bolinder, M.A.; Crotty, F.; Elsen, A.; Frac, M.; Kismányoky, T.; Lipiec, J.; Tits, M.; Tóth, Z.; Kätterer, T. The effect of crop residues, cover crops, manures and nitrogen fertilization on soil organic carbon changes in agroecosystems: A synthesis of reviews. *Mitig. Adapt. Strateg. Glob. Change* **2020**, *25*, 929–952. [CrossRef]
77. Gross, A.; Glaser, B. Meta-analysis on how manure application changes soil organic carbon storage. *Sci. Rep.* **2021**, *11*, 5516. [CrossRef]
78. Liang, S.; Sun, N.; Wang, S.; Colinet, G.; Longdoz, B.; Meersmans, J.; Wu, L.; Xu, M. Manure amendment acts as a recommended fertilization for improving carbon sequestration efficiency in soils of typical drylands of China. *Front. Environ. Sci.* **2023**, *11*, 1173509. [CrossRef]
79. VandenBygaart, A.J.; Gregorich, E.G.; Angers, D.A.; Bolinder, M.A.; Janzen, H.H.; Campbell, C.A. Modeling soil organic carbon change in Canadian agroecosystems: Testing the introductory carbon balance model. In *Soil Carbon Sequestration and the Greenhouse Effect*; Lal, R., Follett, R., Eds.; SSSA Special Publication 57; Soil Science Society of America: Madison, WI, USA, 2009; pp. 13–28.
80. Panagos, P.; Ballabio, C.; Yigini, Y.; Dunbar, M.B. Estimating the soil organic carbon content for European NUTS2 regions based on LUCAS data collection. *Sci. Total Environ.* **2013**, *442*, 235–246. [CrossRef]
81. Yan, D.; Li, J.; Pei, J.; Cui, J.; Nie, M.; Fang, C. The temperature sensitivity of soil organic carbon decomposition is greater in subsoil than in topsoil during laboratory incubation. *Sci. Rep.* **2017**, *7*, 5181. [CrossRef]
82. Schimel, J.P. Life in dry soils: Effects of drought on soil microbial communities and processes. *Annu. Rev. Ecol. Evol. Syst.* **2018**, *49*, 409–432. [CrossRef]
83. Plante, A.; Conant, R.T. Soil organic matter dynamics and climate change effects. In *Global Environmental Change*; Freedman, B., Ed.; Springer: Dordrecht, The Netherlands, 2014; pp. 317–323.
84. Schimel, J.; Balser, T.C.; Wallenstein, M. Microbial stress-response physiology and its implications for ecosystem function. *Ecology* **2007**, *88*, 1386–1394. [CrossRef] [PubMed]
85. Asensio, D.; Zuccarini, P.; Ogaya, R.; Marañón-Jiménez, S.; Sardans, J.; Peñuelas, J. Simulated climate change and seasonal drought increase carbon and phosphorus demand in Mediterranean forest soils. *Soil Biol. Biochem.* **2021**, *163*, 108424. [CrossRef]
86. Naipal, V.; Ciais, P.; Wang, Y.; Lauerwald, R.; Guenet, B.; Van Oost, K. Global soil organic carbon removal by water erosion under climate change and land use change during AD 1850–2005. *Biogeosciences* **2018**, *15*, 4459–4480. [CrossRef]
87. Meersmans, J.; Martin, M.P.; Lacarce, E.; Orton, T.G.; Jolivet, C.C.; Boulonne, L.; Arrouays, D. A high resolution map of French soil organic carbon. *Agron. Sustain. Dev.* **2012**, *32*, 841–851. [CrossRef]
88. Martin, M.P.; Wattenbach, M.; Smith, P.; Meersmans, J.; Jolivet, C.; Boulonne, L.; Arrouays, D. Spatial distribution of soil organic carbon stocks in France. *Biogeosciences* **2011**, *8*, 1053–1065. [CrossRef]
89. Wang, Y.; Weng, B.; Tian, N.; Zhong, Z.; Wang, M. Soil organic carbon stocks of citrus orchards in Yongchun County, Fujian Province, China. *Pedosphere* **2017**, *27*, 985–990. [CrossRef]
90. Mohamad, R.S.; Verrastro, V.; Al Bitar, L.; Roma, R.; Moretti, M.; Al Chami, Z. Effect of different agricultural practices on carbon emission and carbon stock in organic and conventional olive systems. *Soil Res.* **2016**, *54*, 173–181. [CrossRef]
91. Gómez, J.A.; Guzmán, G.; Vanwalleghem, T.; Vanderlinden, K. Spatial variability of soil organic carbon stock in an olive orchard at catchment scale in Southern Spain. *Int. Soil Water Conserv. Res.* **2023**, *11*, 311–326. [CrossRef]

92. Follett, R.F. Soil management concepts and carbon sequestration in cropland soils. *Soil Tillage Res.* **2001**, *61*, 77–92. [CrossRef]
93. van Niekerk, J.M.; Calitz, F.J.; Halleen, F.; Fourie, P.H. Temporal spore dispersal patterns of grapevine trunk pathogens in South Africa. *Eur. J. Plant Pathol.* **2010**, *127*, 375–390. [CrossRef]
94. Elena, G.; Luque, J. Pruning debris of grapevine as a potential inoculum source of *Diplodia seriata*, causal agent of Botryosphaeria dieback. *Eur. J. Plant Pathol.* **2016**, *144*, 803–810. [CrossRef]
95. Vicente-Vicente, J.L.; García-Ruiz, R.; Francaviglia, R.; Aguilera, E.; Smith, P. Soil carbon sequestration rates under Mediterranean woody crops using recommended management practices: A meta-analysis. *Agric. Ecosyst. Environ.* **2016**, *235*, 204–214. [CrossRef]
96. Aguilera, E.; Lassaletta, L.; Gattinger, A.; Gimeno, B.S. Managing soil carbon for climate change mitigation and adaptation in Mediterranean cropping systems: A meta-analysis. *Agric. Ecosyst. Environ.* **2013**, *168*, 25–36. [CrossRef]
97. Rodrigues, L.; Hardy, B.; Huyghebaert, B.; Fohrafellner, J.; Fornara, D.; Barančíková, G.; Bárcena, T.G.; De Boever, M.; Di Bene, C.; Feizienė, D.; et al. Achievable agricultural soil carbon sequestration across Europe from country-specific estimates. *Glob. Change Biol.* **2021**, *27*, 6363–6380. [CrossRef]
98. Berthelin, J.; Laba, M.; Lemaire, G.; Powlson, D.; Tessier, D.; Wander, M.; Baveye, P.C. Soil carbon sequestration for climate change mitigation: Mineralization kinetics of organic inputs as an overlooked limitation. *Eur. J. Soil Sci.* **2022**, *73*, e13221. [CrossRef]
99. Baveye, P.C.; Schnee, L.S.; Boivin, P.; Laba, M.; Radulovich, R. Soil organic matter research and climate change: Merely restoring carbon versus restoring soil functions. *Front. Environ. Sci.* **2020**, *8*, 579904. [CrossRef]
100. Sun, W.; Canadell, J.G.; Yu, L.; Yu, L.; Zhang, W.; Smith, P.; Fischer, T.; Huang, Y. Climate drives global soil carbon sequestration and crop yield changes under conservation agriculture. *Glob. Change Biol.* **2020**, *26*, 3325–3335. [CrossRef]
101. Sánchez-Navarro, V.; Zornoza, R.; Faz, Á.; Fernández, J.A. Comparison of soil organic carbon pools, microbial activity and crop yield and quality in two vegetable multiple cropping systems under Mediterranean conditions. *Sci. Hortic.* **2020**, *261*, 109025. [CrossRef]
102. Thapa, V.R.; Ghimire, R.; Duval, B.D.; Marsalis, M.A. Conservation systems for positive net ecosystem carbon balance in semiarid drylands. *Agrosyst. Geosci. Environ.* **2019**, *2*, 1–8. [CrossRef]
103. McClelland, S.C.; Paustian, K.; Schipanski, M.E. Management of cover crops in temperate climates influences soil organic carbon stocks: A meta-analysis. *Ecol. Appl.* **2021**, *31*, e02278. [CrossRef] [PubMed]
104. Briones, M.J.I.; Schmidt, O. Conventional tillage decreases the abundance and biomass of earthworms and alters their community structure: A global meta-analysis. *Glob. Change Biol.* **2017**, *23*, 4396–4419. [CrossRef]
105. Kabir, Z. Tillage or no-tillage: Impact on mycorrhizae. *Can. J. Plant Sci.* **2005**, *85*, 23–29. [CrossRef]
106. Erickson, A.E. Tillage effects on soil aeration. In *Soil Management: Building a Stable Base for Agriculture*; Lal, R., Stewart, B.A., Eds.; CRC Press: Boca Raton, FL, USA, 2015; pp. 91–104.
107. Zhao, P.; Li, S.; Wang, E.; Chen, X.; Deng, J.; Zhao, Y. Tillage erosion and its effect on spatial variations of soil organic carbon in the black soil region of China. *Soil Tillage Res.* **2018**, *178*, 72–81. [CrossRef]
108. Jin, H.; Huang, S.; Shi, D.; Li, J.; Li, Y.; Zhu, H. Effects of different tillage practices on soil stability and erodibility for red soil sloping farmland in Southern China. *Agronomy* **2023**, *13*, 1310. [CrossRef]
109. AEMET. *Mapas Climáticos de España (1981–2010) y ETo (1996–2016)*; Agencia Estatal de Meteorología: Madrid, Spain, 2018.
110. Wösten, J.H.M.; Lilly, A.; Nemes, A.; Le Bas, C. Development and use of a database of hydraulic properties of European soils. *Geoderma* **1999**, *90*, 169–185. [CrossRef]
111. Shirato, Y.; Yokozawa, M. Applying the Rothamsted carbon model for long-term experiments on Japanese paddy soils and modifying it by simple tuning of the decomposition rate. *Soil Sci. Plant Nutr.* **2005**, *51*, 405–415. [CrossRef]
112. Oficina de Gestión Técnica del Parc Natural de L'Albufera. *Importancia del Cultivo del Arroz en el Parc Natural de L'Albufera*; Generalitat Valenciana, Conselleria de Medi Ambient: Valencia, Spain, 2002.